X-ray Photoelectron Spectrometer Calibration and Thin Film Investigations on Germanium oxides.

T. Deegan, B.Sc.

M.Sc., 1998.

Dublin City University

Supervisor Dr. G. Hughes

School of Physical Sciences

I hereby certify that this material, which I now submit for assessment on the programme of study leading to the award of Masters of Science is entirely my own work and has not been taken from the work of others save and to the extent that such work has been cited and acknowledged within the text of my work.

Signed: Terri Deegan. ID No.: 95970029.

Date: 10th August 1998.

Abstract

The first aim of this project was the characterisation of the VG Scientific Clam100 based, XPS (X-ray Photoelectron Spectroscopy) Spectrometer in the Physics department at Dublin City University Detailed energy scale and intensity scale calibrations were carried out using sputter-cleaned Au (Gold), Ag (Silver), Cu (Copper) and Pd (Palladium) foil samples Analysis of these calibration spectra against standard reference spectra led to an accurate energy calibration and the production of individual transmission functions for the Al Kα and Mg Kα x-ray radiation sources Reference spectra for both energy and intensity calibration were taken from the VAMAS, Versailles project on Advanced Materials and Standards, spectra library

The second part of the project was carried out in the area of thin film thickness determination, namely native oxide on germanium(100) and Ge(111) surfaces An XPS study of the removal of the native oxides from these surfaces by a hydrofluoric (HF) acid based etch treatment was also completed By consistently curve-fitting the chemically shifted oxide peaks for the Ge 3d and Ge $2p_{3/2}$ core levels it was possible to accurately determine the thickness of the residual oxide coverage on the chemically etched surfaces Comparison of oxide re-growth rates with previously reported work for hydrogen passivated silicon surfaces suggests that the chemical etch used on germanium resulted in the formation of hydrogen terminated surfaces

Acknowledgements

I'd like to thank everyone at D C U for their friendship and support during my time there, especially my supervisor, Greg Hughes, for his patience and understanding To Sean and Phil for sharing a lab with me and keeping me laughing along with Eilish, Paul, Colm, Tony and Justin, all members of the Surface Science group and not forgetting Penny and Antoinette from next door

Table of Contents

Chapter 1 Introduction

1.1 Project Aims

The first part of this thesis sets out to characterise an x-ray photoelectron spectroscopy system with the objective of allowing accurate quantitative surface chemical analysis studies to be carried out using this system The technique under investigation is x-ray Photoelectron Spectroscopy (XPS), the system is based on the VG Scientific Clam100 spectrometer XPS is an important surface analysis technique which can be used for both qualitative and quantitative surface characterisation An accurately calibrated system is essential in obtaining useful quantitative information about the surface under investigation Once the system has been calibrated and the procedure is repeated at regular intervals during the system's lifetime, accurate quantitative information can be determined from the XPS spectral data for every suitable material studied

In order to achieve this objective, the initial part of the project focused on obtaining accurate energy and intensity scale calibrations for the VG Scientific Clam100 x-ray photoelectron spectrometer Standard metal foil samples of copper, silver and gold were argon ion bombarded in-situ, to ensure the cleanliness of the surfaces and spectral data over the full energy range was collected These spectra were used in combination with known standard spectra for these metals, obtained from the VAMAS library [1],[2] to produce an accurate energy calibration and transmission functions for the electron energy analyser

Once the system characterisation was completed, an XPS study of the native oxide removal from Germanium (100) and (111) surfaces was carried out Various wet chemical treatments were investigated with the most effective oxide removal treatment being based on a cyclical water rinse / hydrofluoric acid (HF) etch An accurate method of determining the native oxide film thickness was established based on consistently curve fitting the chemically shifted components of the Ge 2p and Ge 3d core levels This method is also applicable to the chemically treated Ge samples and allows the calculation of surface oxide re-growth rates on both the (100) and (111) surfaces

Comparison of the thin film thicknesses with literature values from similarly treated silicon samples suggests that the etched germanium surfaces are hydrogen terminated This layer acts as an effective passivating layer preventing further oxidation of the surface and Ge surfaces prepared in this way are highly stable over extended periods of time

1.2 Thesis Layout

The thesis beings with an introduction to the technique of x-ray photoelectron spectroscopy in Chapter 2, giving the reader a grounding for future chapters The basic XPS system is described in Chapter 3, with a listing of the Clam100 instrumentation

Spectrometer calibration is summarised in Chapter 4 which gives an introduction to the methods used to calibrate the energy and intensity scales and goes on to list results obtained for the Clam100 system Chapter 5 gives details on the estimation of electron escape depths for the various core levels of germanium and the various methods of determining oxide film thicknesses Results of a chemical etching study on the Ge (100) and Ge (111) surfaces are presented in Chapter 6, along with a comparison of oxide removal using argon ion bombardment Chapter 7 contains conclusions and suggestions for future work

1.3 References

[1] VAMAS, Versailles project on Advanced Materials and Standards, The Common Data Processing System, Version 3 1

[2] J Vac Sci Tech JVST A - Vacuum, Surfaces and Films, Vol 10, Nr 6, (1994)

Chapter 2 X-ray Photoelectron Spectroscopy (XPS)

2.1 Introduction

X-ray photoelectron spectroscopy has become one of the most widely used modern day surface analysis techniques, since its development by Kai Siegbahn et al [1] in Sweden in the 60's XPS is based on the photoelectric effect in which a material is irradiated by X-rays of a fixed energy hv These incident x-rays penetrate into the solid and can cause core level electrons to be ejected from the material provided that the x-ray photoelectron energy exceeds the electron binding energy in the solid With reference to Figure 2 1, energy is conserved in the system and so we have the following equation, known as the Einstein equation

$$hv + E'_{Tot} = E_{Kin} + E^{f}_{Tot}(k) \qquad (1)$$

where h^{ν} is the energy of the incident x-rays, E'_{Tot} is the total energy of the initial state, E_{Kin} is the kinetic energy of the ejected photoelectron and E^{f}_{Tot} is the total final energy of the system after the ejection of the photoelectron from the k^{th} level [2]

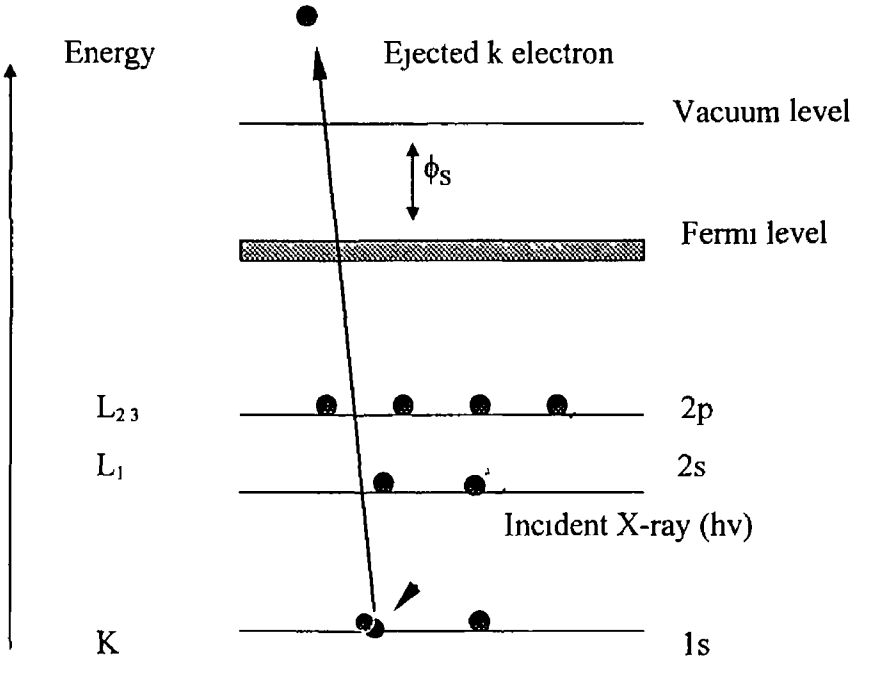

Figure 2.1 · X-ray photoelectron spectroscopy

In Figure 2 1, ϕ_S is defined as the workfunction The binding energy (B E) of the photoelectron is the energy required to remove it to infinity with a zero kinetic energy For, XPS, $E_B^F(k)$, the B E of an electron in the k^{th} level, is defined as

$$E_B^F(k) = E^f_{Tot} - E^i_{Tot} \qquad (2)$$

So substituting this into the energy conservation equation gives us

$$hv = E_{Kin} + E_B^F(k) \qquad (3)$$

Binding energy is expressed relative to a reference level, which is the Fermi level, in the study of solids For a solid sample, there is electrical contact to the spectrometer For metallic (conductive) samples, the resulting energy levels are shown in Figure 2 2

Figure 2 2 XPS Energy level diagram for conductive samples

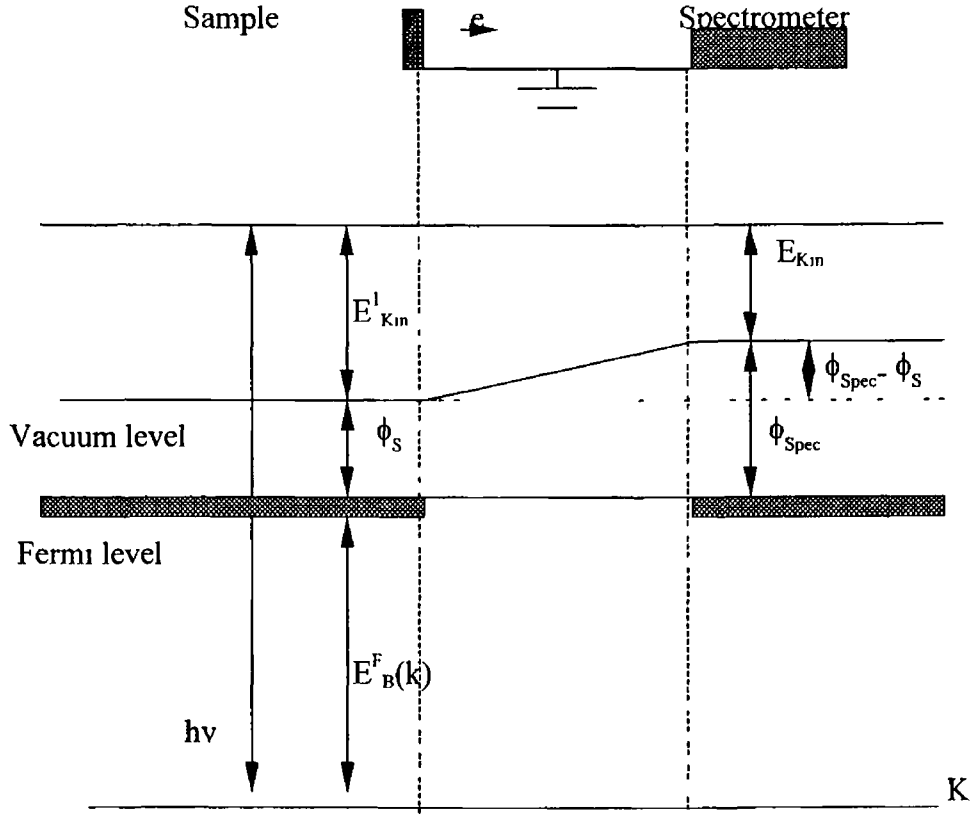

The sample and spectrometer are at equilibrium and therefore their Fermi levels are equal A photoelectron passing from the sample surface into the spectrometer will experience a potential difference equal to the difference between the two workfunctions, φ_{Spec} and φ_S

The electron kinetic energy E^1_{Kin} at the sample surface is measured as E_{Kin} inside the spectrometer analyser

$$E_{Kin} = E^1_{Kin} + (\varphi_S - \varphi_{Spec}) \quad (4)$$

Referring to Figure 2 2, the energy conservation equation is now

$$h\nu = E_B^F(k) + E_{Kin} + \varphi_{Spec} \quad (5)$$

which is more commonly expressed in the form

$$E_{KE} = h\nu - E_{BE} - \varphi \quad (6)$$

where φ is simply the workfunction term [2]

With XPS, electrons are ejected from particular core levels (the s, p, d, f subshells), that is they have certain well-defined binding energies They therefore have correspondingly well-defined kinetic energies when ejected The experimental determination of this energy distribution N(E), by a kinetic energy analysis of the photoelectrons produced following x-ray irradiation is termed X-ray photoelectron spectroscopy (XPS) Figure 2 3 shows the typical XPS spectrum for a gold foil sample, with the different peaks corresponding to electrons photoejected from the different core levels of the material in question

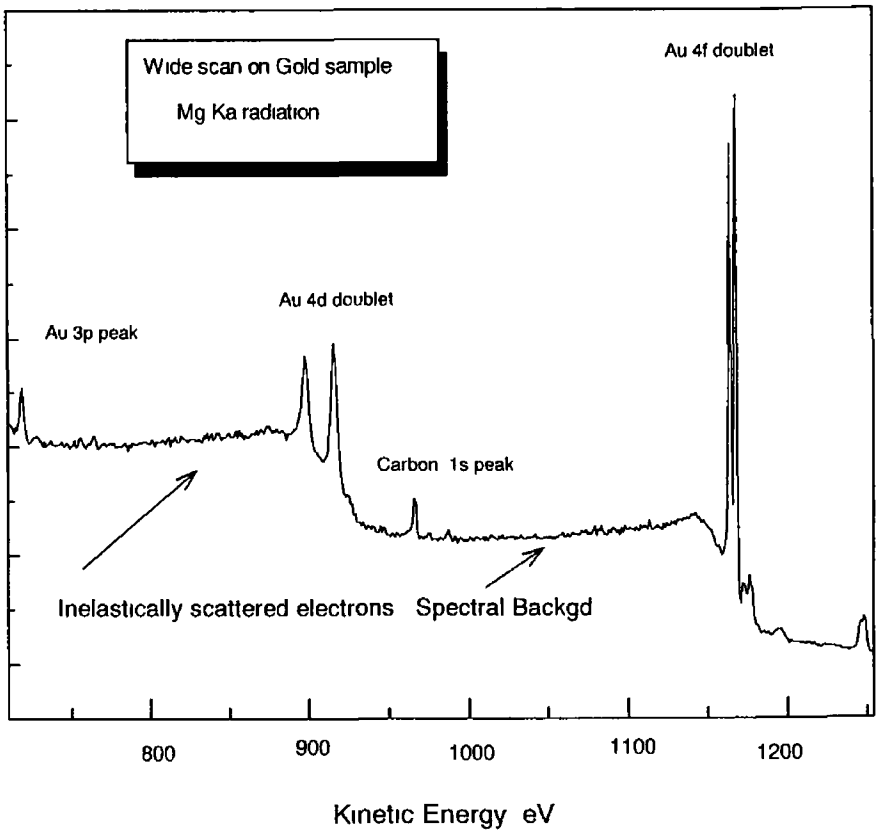

Figure 2.3 : Typical XPS spectrum for an untreated gold sample Survey scan showing Au peaks, carbon contamination on the surface and the inelastic background

2.2 Photoionisation Cross-sections

The number of photoelectrons produced from any given core level of an element is determined by the photoionisation cross-section (σ) of that level for the photon energy ($h\nu$) concerned σ is defined as the transition probability per unit time for excitation of a single photoelectron from the core level of interest under an incident photon flux of 1 $cm^2 s^1$ [3]

The photoionisation cross-sections for all elements at 1254 eV and 1487 eV, the two principal x-ray sources lines used (Mg Kα and Al Kα respectively), were calculated by Scofield, with every element being referenced against the C 1s peak which has a cross-section of 1 [4] The Scofield table is widely used to extract quantitative

information from XPS spectra and hence characterise the surface under investigation Once the individual peaks have been identified and the photoionisation cross-sections looked up in the Scofield table for each of the elements present, the elemental composition can then be determined, as follows

$$\text{Peak Height / Cross-section}$$

$$\text{Sum of all peak intensities} = 100\%$$

$$\text{Fractional \%} = \text{individual peak intensity / 100}$$

2.3 Inelastic Scattering and Sampling Depth

Following photoionisation, the photoelectron of energy E_{KE} , must travel through the solid and escape into the vacuum, "without losing energy" , before it can be analysed and detected as a characteristic photoelectron The incident x-rays can penetrate to a depth of several microns or roughly 500 atomic layers, whereas electrons in the energy range 50-1000 eV typically travel only 2-10 atomic layers before losing energy through inelastic scattering events in the solid Electrons which lose energy in this way cannot contribute to the characteristic photoelectron peak at energy E_{KE}, and become part of the XPS spectrum background [3] This background is also visible in the gold spectrum shown in Figure 2 3

The probability of an inelastic scattering event occurring is determined by both the electron energy and the material through which it is travelling Since it is a random process governed by probability, inelastic scattering is described by the standard exponential decay law

$$I(x) = I_0 \exp(-x / \lambda(E_k,Z) \ \cos\theta) \qquad (7)$$

where I_0 is the original photoelectron intensity, I(x) is the intensity remaining after travelling through a material of thickness x, θ is the angle of emission with respect to the surface normal and $\lambda(E_k,Z)$ is termed the electron escape depth (ED) and represents the depth at which photoelectrons have a probability of 1/e of escaping without energy loss

2.4 The Universal Curve

There is a so-called universal curve as shown in Figure 2 4, which has been produced by plotting a range of experimentally determined escape depths as a function of kinetic energy [5]

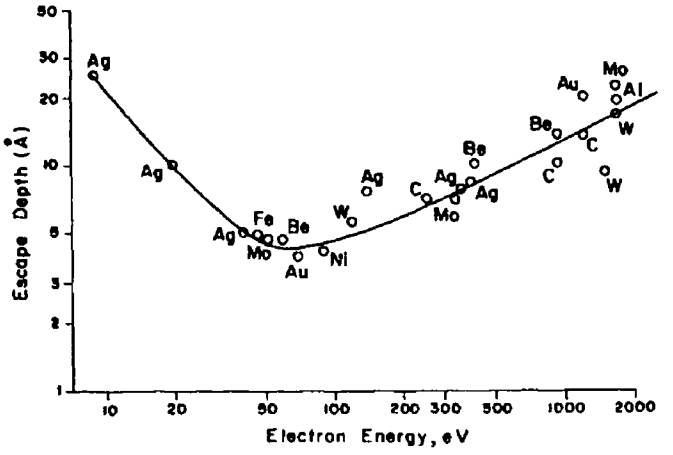

Figure 2 4 · The Universal Curve Electron escape depth versus kinetic energy in metals

Although, this curve can provide a general indication of escape depth at a particular energy value it makes the assumption that λ is independent of the material (Z) in which it travels, which is untrue Knowledge of the exact escape depth, λ, for a particular material (Z) is an important requirement for quantitative XPS analysis Many formulae to estimate λ have been developed over the years and these are discussed in greater detail in chapter 5 In general, the sampling depth d, of XPS is taken as ~ 3λ, due to the exponential nature of the I(x) equation, it is easy to show that 95% of the signal detected originates from a sampling depth equal to 3λ Variations in sampling depth with kinetic energy and with emission angle θ can be exploited and lead to two separate forms of XPS analysis One in which the variation in λ with K E is utilised known as Kinetically Resolved XPS (KRXPS), [6] and the other in which the angular variation is used, known as Angular Resolved XPS (ARXPS) [3]

2.5 The Chemical Shift

The binding energy of an electron is dependent on its chemical environment The energy of an electron in a core level is determined by its Coulomb interaction with the other electrons and also by its attraction to the positively charged nucleus A change in the chemical environment of the element will lead to a redistribution of its valence electron charges and so the core electrons will experience a different potential i e its binding energy will change For certain elements this B E change is clearly identifiable in the XPS spectrum and is known as the chemical shift The existence of this chemical shift leads to many more applications as XPS analysis can identify the elements present in a given sample and also provide information as to the chemical environment of these surface atoms

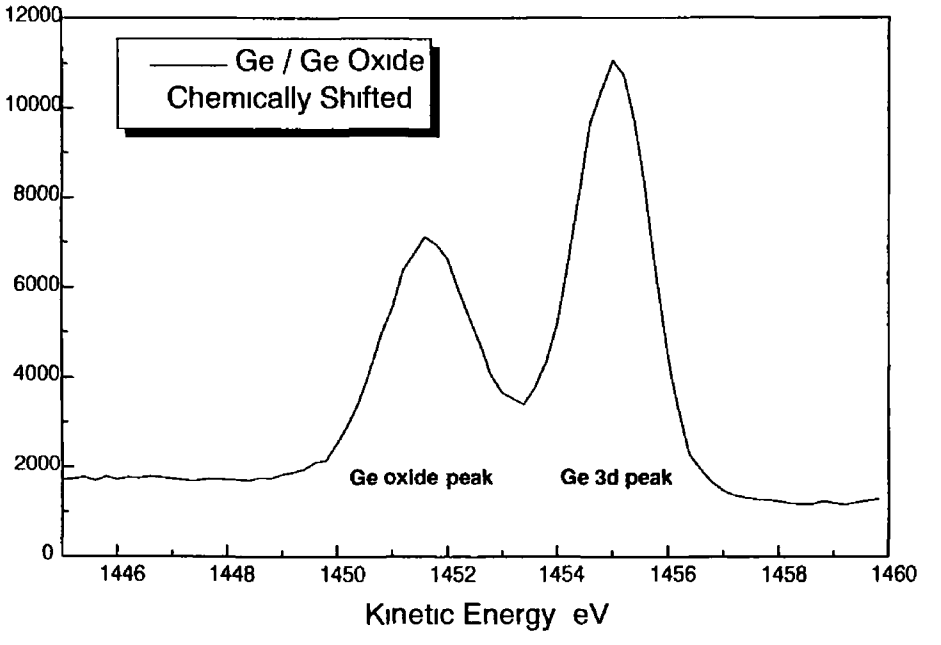

Figure 2.5 An example of how the chemical shift can identify elements in different bonding environments, here Ge and GeO_2 shifted by 4 eV It also displays quantitative information, as the size of the peaks directly relates to the number of atoms in their different chemical environments

2.6 Conclusion

This chapter serves as an introduction to the theory behind X-ray Photoelectron Spectroscopy and some of it's most important concepts XPS can be used to identify all elements present on a surface (excepting hydrogen) and through use of the chemical shift phenomena, knowledge of their chemical bonding environment is also gained Quantitative information is easily obtained through the use of the existing data tables of Scofield to yield elemental concentrations as an atomic % Clearly, it is very important to quantify the concentrations of the elements present on the surface under investigation, as well as being able to identify them individually In order to ensure the validity of results obtained the XPS system must be properly calibrated and this is discussed in Chapter 4

2.7 References

[1] K Siegbahn, C Nordling, A Fahlman, R Nordberg, K Hamrin, J Hedman, G.Johansson, T Bergmark, S E Karlsson, I Lindgren and B Lindberg, ESCA - Atomic, Molecular and Solid State Structure Studied by Means of Electron Spectroscopy, Almquist and Wiksells, Uppsala, 1967

[2] Leonard C Feldman and James W Mayer, Fundamentals of Surface and Thin Film Analysis, North-Holland

[3] A B Christie, Ch 5, Methods of Surface Analysis, Editor J M Walls, Cambridge University Press [Pg 152]

[4] J H Scofield, J of Electron Spectro and Related Phenomena, (1976), 129-137

[5] W M Riggs and M.J Parker, Methods of Surface Analysis, Editor A W Czanderna, Elsevier

[6] Yu Wie, John L Sullivan and Sayah O Said, Vacuum, Vol 45, 5 (1994), 597-601

Chapter 3 Instrumentation

3.1 The UHV environment

The basic elements of an x-ray photoelectron spectrometer are shown below An intense beam of x-rays must be produced, hit the target sample and cause core electrons to photoeject These photoelectrons must enter an energy analyser which is coupled to an electron detector that can provide a suitable output signal for display purposes

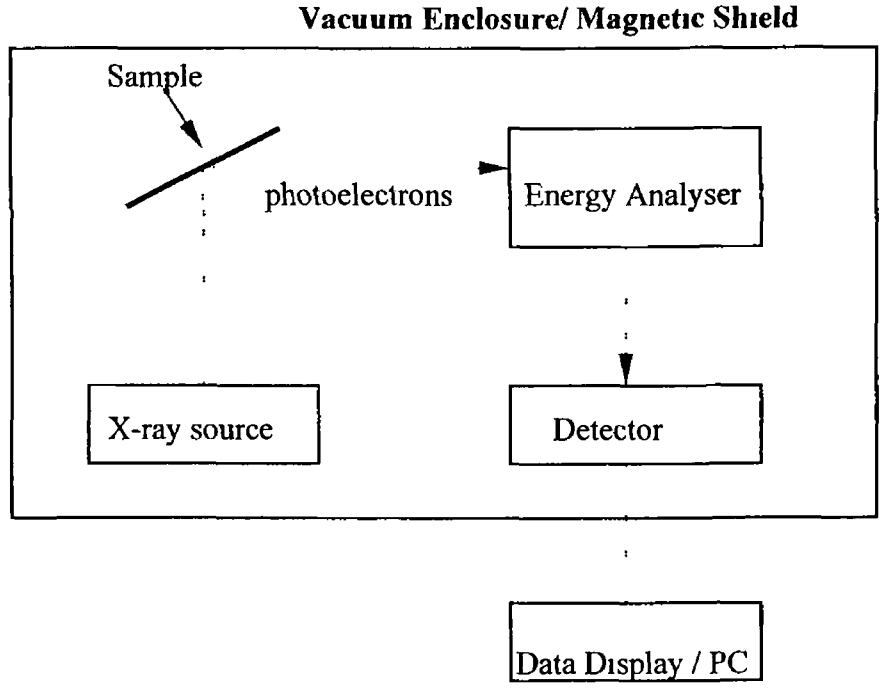

Figure 3 1 The basic elements of an X-ray photoelectron spectrometer [1]

The vacuum environment serves two purposes, it maintains the sample chamber and analyser at a sufficiently low pressure so that the photoelectrons have a long mean free path relative to the internal dimensions of the spectrometer (i e so that they can be detected before scattering) Secondly it reduces the partial pressure of reactive residual gases, preventing contamination of the sample surface [1] Many systems also contain a mass spectrometer to monitor the levels of the gases present and to detect leaks The vacuum used in these studies employs an ion pump and turbomolecular pump backed by a rotary pump The UHV pumping arrangement used is shown in Figure 3 2

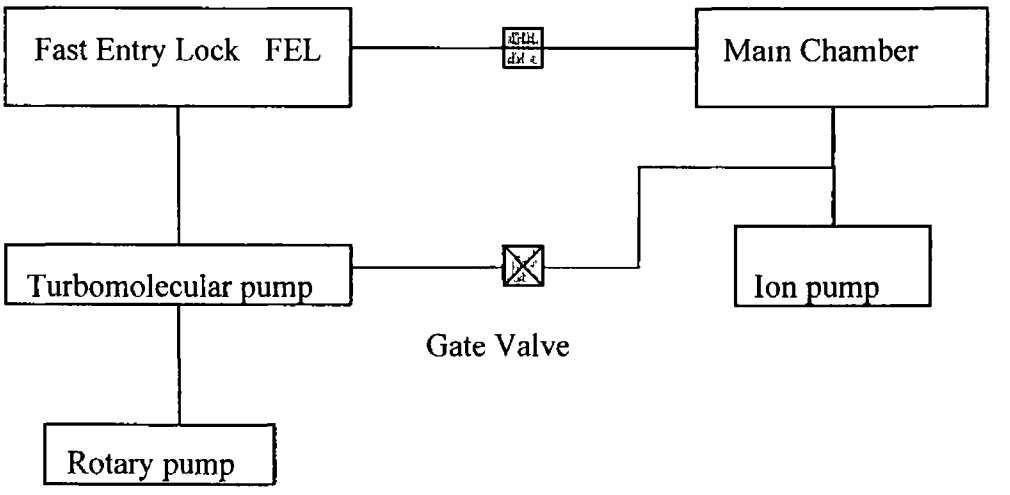

Figure 3 2 The UHV pumping arrangement in block diagram form

The UHV system used consists of a stainless steel cylindrical main chamber 12 in diameter and 18 in height, with top and base ports of 6 and 8 diameter, respectively The XYZ manipulator is located at the top port while the base port is connected to the ion pump, which leads through a 6 gate valve to the turbomolecular pump The main working level contains five 2 ¾ ports, four of which are at right angles to each other Three of the other ports are viewing ports while a VG ion gauge is fitted to the fourth port to monitor the pressure in the main chamber Base pressures of 10^{10} mbar were achieved in the main chamber following a 24 hour bake-out at 180° C The fifth port is connected to the fast entry lock which can be valved off to allow samples to be inserted These samples can then be transferred onto an internal 4-way cross-arm in the main chamber and positioned in front of the energy analyser entrance

3.2 The X-ray Source

A basic x-ray source consists of a heated filament and a target anode, as shown in Figure 3 3 A high voltage potential is applied between the filament and the anode to accelerate the electrons emitted from the filament towards the target Electron bombardment of the target anode produces core vacancies and causes the emission of x-rays by fluorescence

These x-rays are characterised by a continuum (termed Bremsstrahlung radiation) upon which is superimposed discrete wavelengths of varying intensity, see for example the Mg K-shell emission shown in Figure 3 4

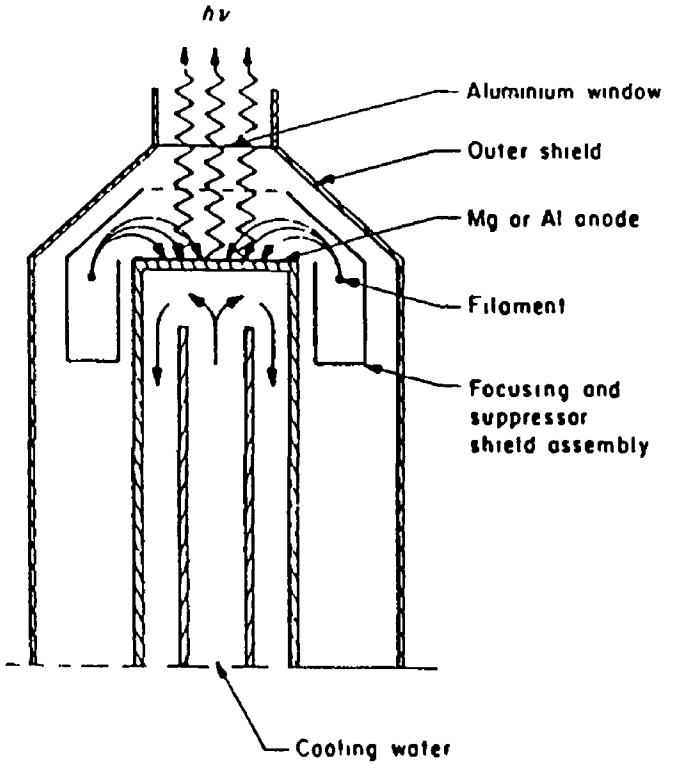

Figure 3.3 · Typical x-ray source innards

The conversion of high voltage electrons into x-rays is an inefficient process (~1% total applied power converted) and most of the electron energy is dissipated as heat It is necessary therefore to water cool the anode The generated x-rays then pass through a thin window and hit the sample surface The window stops scattered electrons in the x-ray source from entering the vacuum chamber and if made from Aluminium (typical for Al/Mg twin source) purifies the x-ray spectrum by absorbing Bremsstrahlung radiation above approximately 1600 eV [1]

In XPS, the most commonly used x-ray source is the twin anode Mg/Al source The Kα doublet of Aluminium has a energy of 1486 6 eV with a composite linewidth of ~ 0 85 eV FWHM The Kα doublet of Magnesium has an energy of 1253 6 eV with a composite linewidth of ~ 0 7 eV FWHM The typical Mg K-shell x-ray emission spectrum is shown in Figure 3 4, with the $K\alpha_{1,2}$ doublet clearly dominant (Note the logarithmic intensity scale)

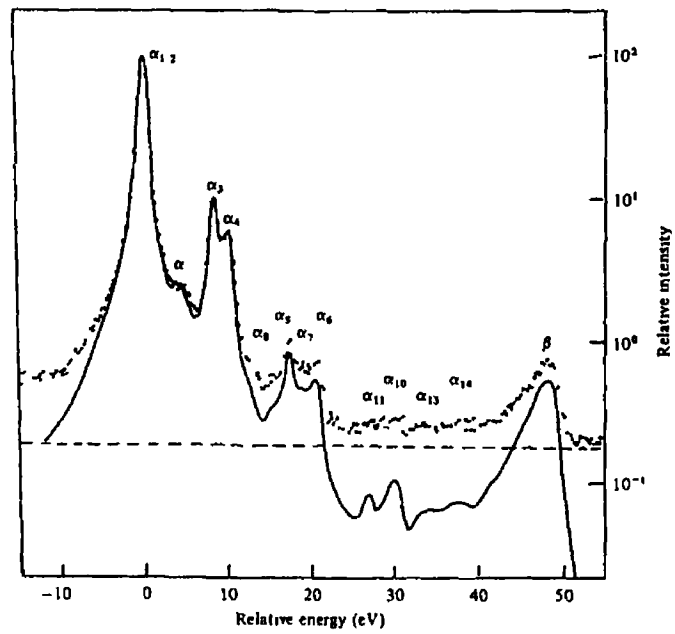

Figure 3 4 : Mg K-shell X-ray emission spectrum The full line shows the characteristic line emission after subtraction of a constant background as shown by the dashed line [2]

Note : Mg/Al x-ray sources are usually both operated at an anode voltage of 15 kV and a current of 20 mA, to produce sufficiently intense photoelectron peaks

3.3 Argon Ion Bombardment

Most samples to be analysed require some form of surface cleaning before attempting XPS One method of preparing the surface is in-situ sputter cleaning using an inert gas ion source Ions are created when electrons from the filament are accelerated across the ionisation chamber containing the inert gas, towards the anode This creates a low pressure plasma The ions are extracted from the cell by applying a negative bias to an extractor lens which focuses the ions into a ~ 10mm diameter spot size at a working distance of ~ 100mm beyond the ion source body Exposing the sample to this ion beam will remove surface contamination at a selectable rate

The Clam100 based system at DCU is fitted with an AS10 sputter cleaning ion source from VSW (Omicron Electron Spectroscopy Ltd) which uses argon ions to sputter-clean samples The argon ion energy is fixed at 500 eV and typical sample currents of $7\mu A/cm^2$ where routinely achieved [3]

3.4 The Electron Energy Analyser

The function of the energy analyser is to measure the number of photoelectrons as a function of their energy i e the spectrum produced shows photoelectron peak intensity versus kinetic energy position There are various types of analysers in use, the most common XPS analyser is the Spherical Sector Analyser (SSA) shown below

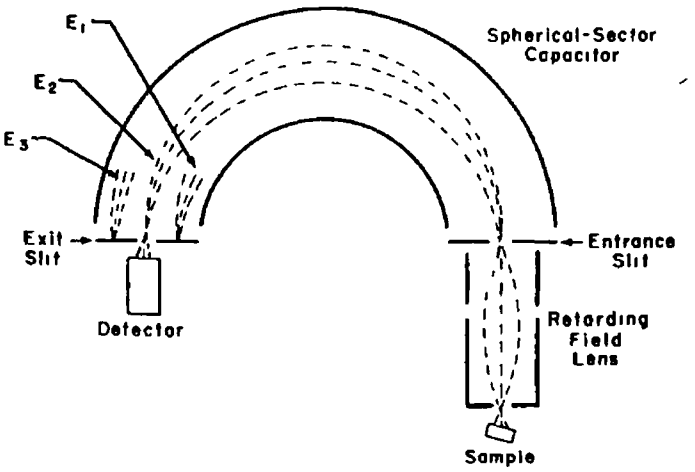

Figure 3.5 · Spherical Sector Analyser geometry [1]

The geometry of the SSA is similar to a prism and lens system Electrons with different energies are separated as they travel through the electric field Electrons with the same energy but diverging from each other will be brought to a focus at the exit slit

A spectrum can be produced by scanning the voltage applied to the hemispherical plates of the analyser such that electrons having successive energies are allowed to pass through the exit slit and reach the detector Alternatively, a fixed voltage is applied to the analyser and the retarding field is scanned Photoelectrons are slowed down by the retarding field and only those electrons that match the sector voltage (pass energy) will reach the detector This mode of analyser operation is known as the constant analyser energy mode, CAE mode The former scanning mode known as the constant retard ratio mode, CRR and produces constant resolving power throughout the spectrum, but instrumental resolution scales with kinetic energy Retardation gives constant resolution across the entire spectrum and better sensitivity to electrons of low initial kinetic energy Throughout this work the analyser was only operated in the CAE mode [1]

3.5 The Transfer Lens

Most systems usually employ some form of transfer lens system in order to distance the spectrometer entrance slit from the sample and allow good access around the sample for example, to position the x-ray source The lens system for the Clam100 consists of two Einzel lenses The lenses are operated at short focal lengths in a "back to back mode" to give unity magnification The use of two lenses at short focal length rather than one single lens gives improved collection efficiency The lens potentials are scanned in proportion to the kinetic energy of the electrons to the analyser Under these conditions the focal length of the lens remains constant, i e there is no change of magnification with kinetic energy Thus the area imaged should remain constant throughout the energy range [4]

3.6 The Electron Detector

The current actually reaching the analyser exit in XPS is typically in the range 10^{-16}-10^{-14} Amps, i e well below conventional current measuring techniques, and pulse counting is the preferred detection method The most commonly used detector is the channel electron multiplier or channeltron The channeltron is an electrostatic device which employs a continuous dynode surface usually in the form of a thin-film conductive layer on the inside of a spiral glass tube Only 2 electrical connections are required to establish the conditions for electron multiplication Typical output pulses are in the range of 10^8 electrons of less than 1μs duration [5]

The final output from the multiplier is a series of pulses that are fed into a dedicated electronic control unit, where it is usually A-to-D converted and transferred to a computer for display Our system uses the commercially available VGX900 computer software acquisition and processing package

Brief Note The sample position and geometry of the x-ray source, sample and analyser input slit are clearly important in obtaining the best XPS spectra It is also desirable to have the sample in electrical contact with the spectrometer to prevent charging effects

3.7 The Clam100 Analyser System

The VG Clam 100 spectrometer **[CLAM Combined Lens Analyser Module]** has a Model 849 analyser, which is a 100mm mean radius of curvature, 150^0 spherical sector analyser fitted with a single channel electron multiplier detector, with four pairs of externally adjustable slits of 4, 2,1 and 0.5 mm (inlet and exit equal) Most work can be done with the 4mm slits and control of resolution can be achieved by varying the pass energy of the analyser The advantage of the smaller slit settings is that some control of the sample area being investigated is achieved The spectrometer control unit incorporates a switch for setting analysing energies of 2, 5, 10, 20, 50, 100 and 200 eV [4] The CLAM100 from VG Scientific at Dublin City University is shown in Figure 3 6

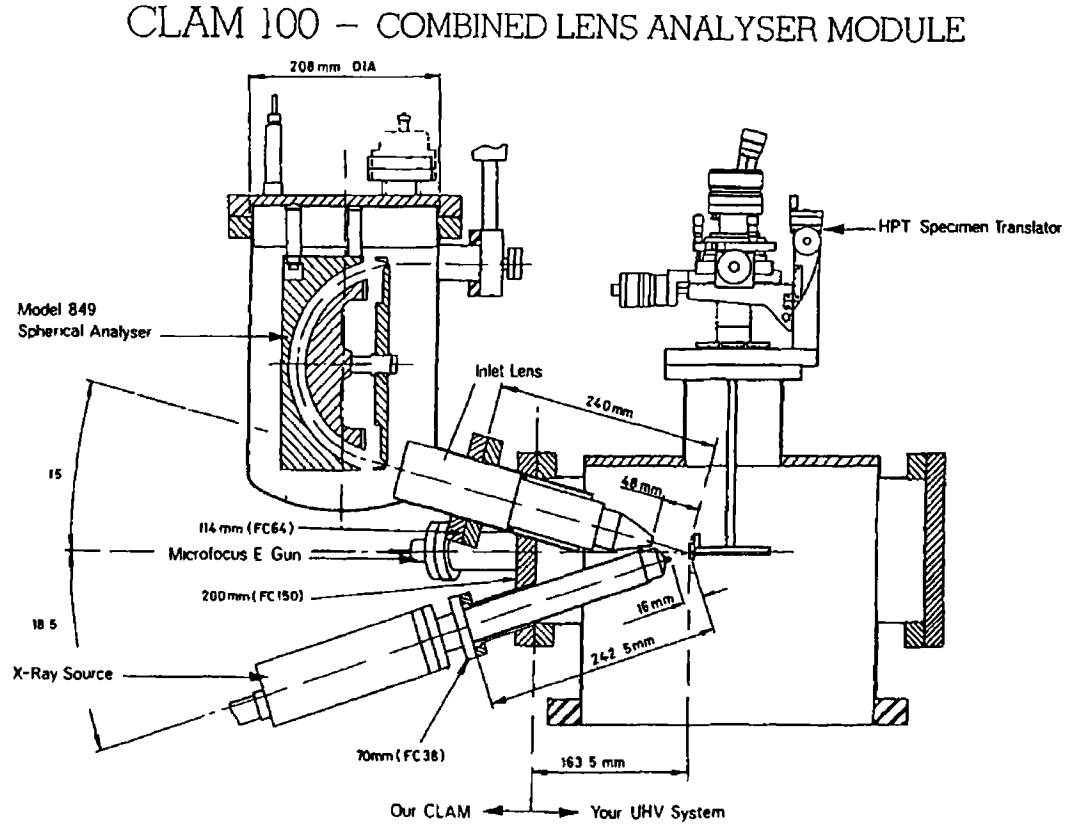

Figure 3 6 Dimensions for Clam mounted on 200mm OD adaptor flange [6]

The analyser is operated in Constant Analyser Energy (CAE) mode, as shown in Figure 3 7 In this mode (ΔE = constant), the analyser acts as a narrow pass filter transmitting electrons with an energy HV where V is the potential difference between the "hemispheres" and H is a constant determined by the physical dimensions of the analyser Electrons from the sample are retarded to an energy HV by a scanned retarding potential R applied between the earthed sample and the electrical centre point of the "hemispheres" The kinetic energy K of an ejected electron (conventionally referred to the Fermi level) is given by

$$K = R + HV + W \qquad (1)$$

where W is the workfunction of the analyser materials [4]

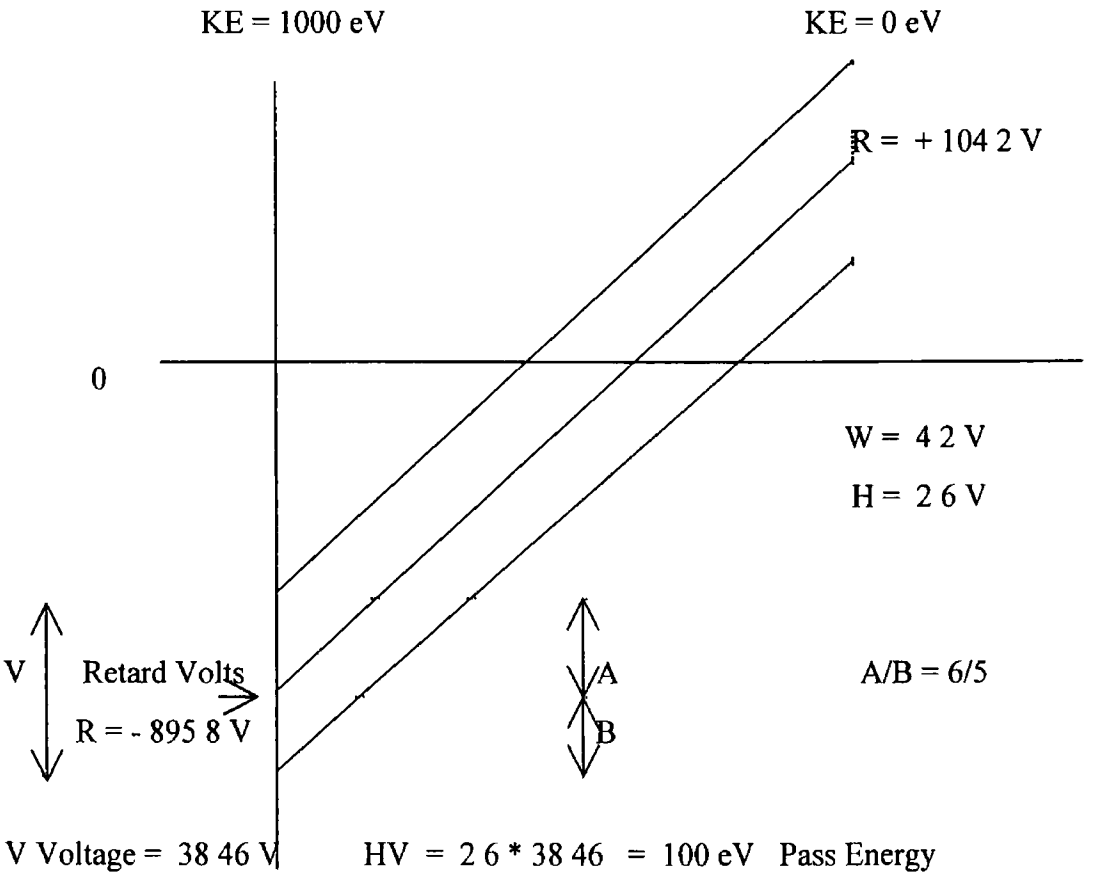

Figure 3 7 · Retard and Hemisphere voltages over range KE = 1000 eV to 0 [4]

In the above description the analyser is referred to as an energy filter, letting through only electrons with an energy, e = HV This is the ideal picture and in practice the analyser energy setting does in fact, effect the resolution The analyser actually lets through electrons in the range, $e \pm de$ and it can be shown that

$$de/e = dr/2r + \alpha^2 \qquad \textit{approximately} \qquad \textbf{(2)}$$

where r is the mean radius of the hemispheres, α is the half angle of admission of electrons (in radians) and dr is the slit width (in the same units as r) Here *de* would be the full width at half height of a recorded peak assuming infinitely small source and specimen line widths, and since for a given geometry *de/e* is constant, *de* will decrease linearly with *e* Thus as we decrease analyser energy we decrease line width and increase resolution (This is ultimately limited by the source and specimen line widths) [4]

Analyser Energy	Line Width at Half Height
(in eV)	(in eV)
10	1 05
20	1 2
50	1 7
100	2 5

Table 3.1 · Clam100 analyser Typical FWHM line widths for Au, *? 4f peaks* at a given analyser energy setting, using the Al Kα source As specified by the manufacturer [4]

The analyser energy setting also effects the sensitivity Sensitivity is approximately proportional to e^2/L^2K This does not imply infinite sensitivity for K = 0, as clearly under the conditions described, $K = e + W$ for electrons to pass through the analyser, where K is the kinetic energy of the photoelectrons (referred to the Fermi level), e is the analyser energy setting (in eV's) and W is the workfunction of the spectrometer [4]

Thus, referred to 100% sensitivity at 100 eV analysing energy for a given value of K

Analyser Energy (eV)	Sensitivity (approximate)
10	6 %
20	17 %
50	54 %
100	100 %

Table 3.2 · Clam100 analyser Typical % sensitivities at a given analyser energy setting As specified by the manufacturer [4]

As is usual, the higher resolutions cannot be obtained without a considerable sacrifice in sensitivity Note that Sensitivity at KE_1 / Sensitivity at KE_2 = KE_2 / KE_1 i e the sensitivity of the instrument increases as the kinetic energy decreases (binding energy increases) Resolution remains constant throughout a scan, at any given energy setting [4]

3.8 Clam 100 Analyser & Channeltron Detector Characterisation

Initially some characterisation work must be carried out in order to ensure that the spectrometer is operated correctly, e g at good resolution and sensitivity settings In the case of the channeltron detector, a certain potential difference must be applied to the channeltron in order to amplify the signal and ensure that all the photoelectrons leaving the analyser are collected Figure 3 8 shows the effect of increasing the applied kV until a certain threshold is reached and the graph levels off Clearly, the applied kV must lie in the plateau region of the graph to ensure correct detector operation

Figure 3 9 shows the effect of varying the analyser slit width on the counts detected The wider the slits, the greater the number of electrons that can pass through the analyser to the detector However, variations in the count rate also affect the energy resolution FWHM, as shown in Table 3 3

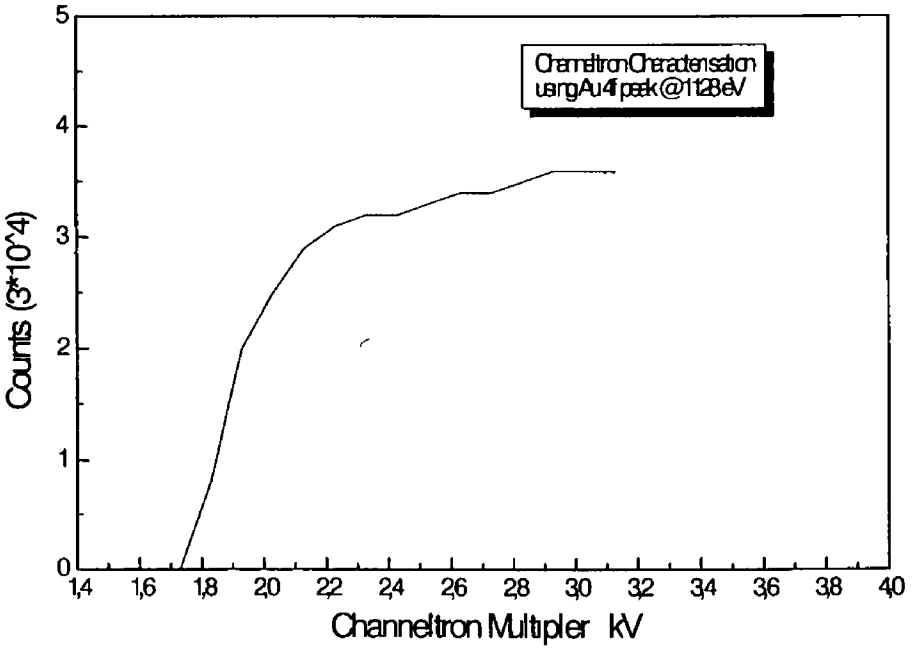

Figure 3.8 · Detector characterisation graph showing counts detected versus kV applied to channeltron multiplier

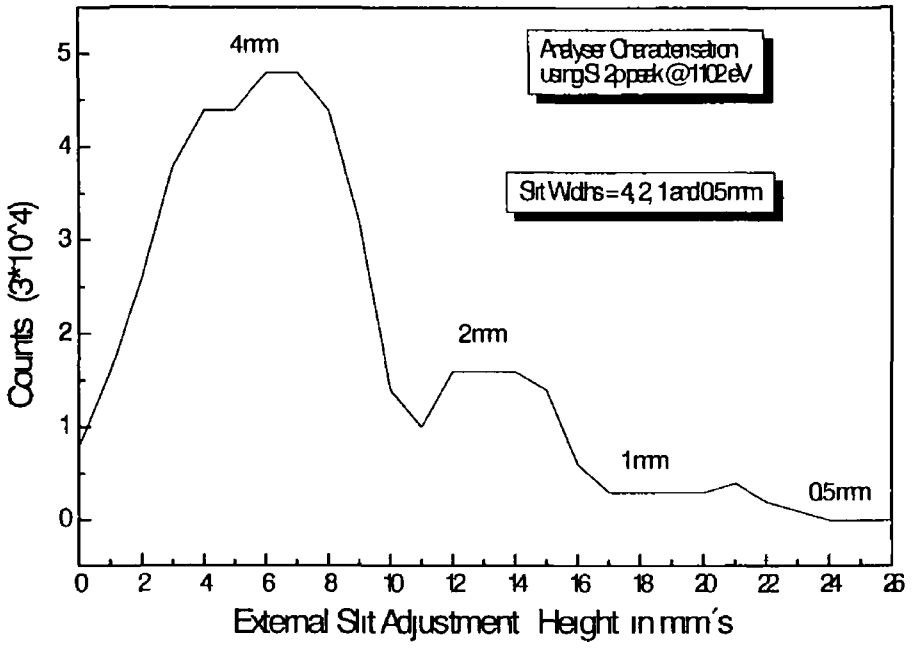

Figure 3.9 Analyser characterisation graph showing counts detected versus slit width

Count Rate (counts per second)	**Energy Resolution FWHM (eV)**
50,000	0 85
80,000	0 90
140,000	1 00
630,000	1 75

Table 3.3 Count Rate versus Energy Resolution as specified for the Clam100 analyser in CAE mode, for the Ag $3d_{5/2}$ peak using 300 Watts Mg Kα radiation

3.9 VGX900 Software

Once the set-up has been properly completed and the sample inserted, scanning can begin Most surface scientists repeat the same scans several times and average the scan data Commercial software packages now exist to record the spectral data and convert it into a suitable display format Most packages can also perform useful functions such as spike removal and differentiation In the course of the studies detailed here the VGX900 software package from VG Scientific was used to collect data [8] Parameters such as start and stop energy, step size, dwell time and number of scans where individually set-up as required, for each of up to 10 separate energy interval regions

3.10 Conclusion

This chapter is concerned with the vacuum system and instrumentation needed to carry out XPS studies The elemental parts such as x-ray source, analyser and electron detector etc were described in detail and the Clam100 based analyser system used in these studies was also discussed The Constant Analyser Energy mode, CAE mode was described and typical % sensitivity factors and full width half maximum values for different analyser energies were given Detector and analyser characterisation was also detailed and the chapter ended with a description of the software package used to collect the spectral data and convert it into a useful format

3.11 References

[1] W M Riggs and M J Parker, Methods of Surface Analysis, Edtr A W Czanderna, Elsevier

[2] D P Woodruff & T A Delchar, Modern Techniques of Surface Analysis, Cambridge

[3] Instruction Manual, AS500F Sputter Cleaning Ion Source, VSW Instruments Ltd

[4] VG Scientific Ltd , as specified in User's Manual

[5] A B Christie, Methods of Surface Analysis, Editor J M Walls, Cambridge University Press

[6] VG Microtech Ltd , Clam 100 Combined Lens Analyser Module, Specifications

[7] VGX900 software manual

Chapter 4 Calibration of Electron Spectrometer

4.1 Energy Scale Calibration

If we wish to use XPS to gain chemical state information (to determine the chemical states present at the sample surface) the exact photoelectron peak position in the energy spectrum must be known Different chemical environments usually cause only small shifts in peak positions of the order of a few electron volts Accurate energy calibration of the spectrometer is therefore essential to obtain quantitative information from XPS spectra

Previously no accepted set of values existed with which to calibrate spectrometers and an accepted reference procedure for calibration was also lacking This led to a range of calibration binding energies being published in the literature [1] To improve the situation the National Physics Laboratory (NPL) in Teddington, England, set up the first traceable reference calibration line energy positions for both XPS & AES, as shown in Table 4 1 below

	Al Kα*	Mg Kα
Cu 3p	75 14 ± 0 02	75 13 ± 0 02
Au $4f_{7/2}$**	83 98 ± 0 02	84 00 ± 0 01
Ag $3d_{5/2}$***	368 26 ± 0 02	368 27 ± 0 01
Cu L_3MM	567 96 ± 0 02	334 94 ± 0 01
Cu $2p_{3/2}$	932 67 ± 0 02	932 66 ± 0 02
Ag M_4NN	1128 78 ± 0 02	895 75 ± 0 02

* Al Kα - Mg Kα = 233 02 eV

** Au $4f_{7/2}$ Al Kα BE lowered by Au $4f_{5/2}$ tail

*** Ag $3d_{5/2}$ Mg Kα BE raised by Ag $3d_{3/2}$ X-ray satellite

Table 4.1 : Reference calibration line energy positions, expressed in eV's [2]

The energy scale is expressed as a binding energy E_B, referenced to the scale position, XFL, of the photoelectrons emitted from the Fermi level (FL) of a metal, as shown in Figure 4.1. Nickel and Palladium are the two elements used in practice to define the XFL reference as there is a high density of occupied states at their Fermi levels. Table 4.1 shows calibration positions, E_B, of sputter-cleaned polycrystalline foils of copper, silver and gold, using unmonochromated Mg Kα and Al Kα radiation. Instruments are usually calibrated using the Au $4f_{7/2}$ and Cu $2p_{3/2}$ peaks at either end of the energy scale.

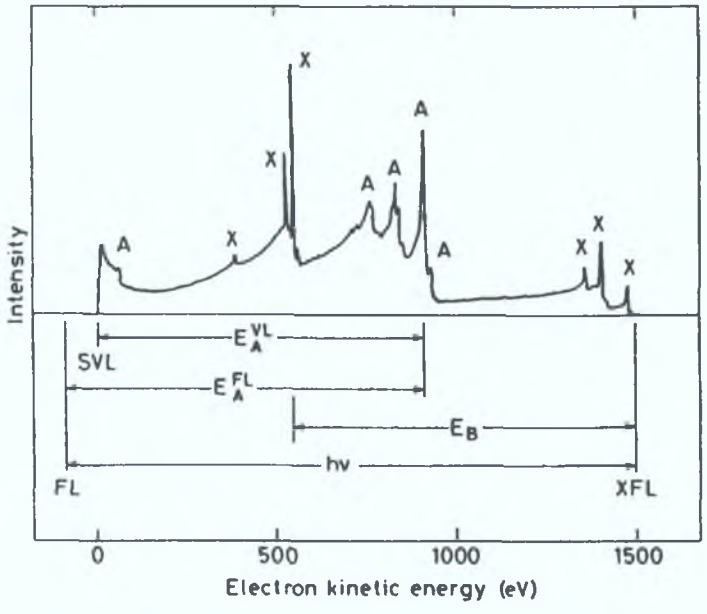

Figure 4.1 : X-ray photoelectron spectrum for copper. The photoelectron peaks are labelled X and the Auger electron peaks A. The positions of the metal Fermi level (FL), the standard vacuum level 4.500 eV above this (SVL) and of the photoemitted Fermi level (XFL) electrons are all indicated. [2].

Note : In their paper on energy scale calibration, Anthony & Seah [1] state that Cu 3p data is not recommended for any high accuracy calibration work due to its weak strength, greater breadth and asymmetry.

Many spectroscopists often use adventitious carbon (AC) as a binding energy standard. As AC is present on all air exposed surfaces it is the simplest method of establishing a standard for studies on non-conductive materials. Barr and Seal have recently reviewed the validity of this approach. [3].

4.2 Clam100 Results

4.2.1 Defining the Reference Zero of Binding Energy

In order to carry out an accurate energy scale calibration, the exact reference zero of the binding energy scale must be known The reference zero is taken as the Fermi level position Any metal can be used to define the reference zero, as all metals in contact will have Fermi levels at the same energy As stated above either Ni or Pd are generally used as they both have Fermi levels in the intense d-band of the conduction electrons and are likely to yield accurate results as the signal strengths will be high

In our case sputter-cleaned Pd foil was used to obtain Fermi edge spectra Spectra were taken using both the Mg Kα and Al Kα sources, at pass energies of 20 eV & 50 eV and covering all slit width settings Theoretically the Fermi edge should be sharply defined as shown in Figure 4 2 below, however broadening distorts the Fermi edge making it more difficult to determine its exact position Previously the Fermi edge was taken as the point on the curve at which the intensity above the background has fallen to 50%, however the peak required at the Fermi edge is given by the differential of the energy spectra which yields the exact reference zero position Figure 4 3 shows Fermi edge spectra obtained using a Pd sample along with the differentials of these spectra

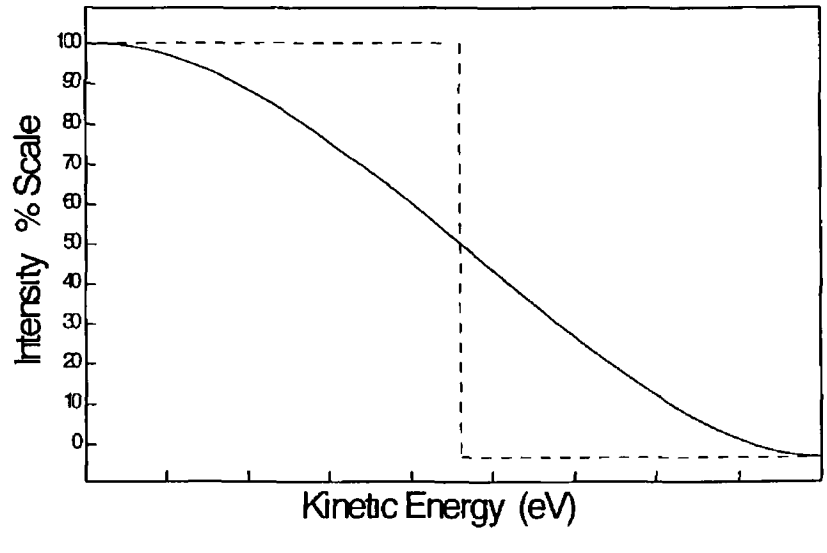

Figure 4.2 . Theoretical (dashed line) vs Experimental (solid line) Fermi edge shapes, to illustrate the need to differentiate Fermi edge spectra to obtain the true reference zero

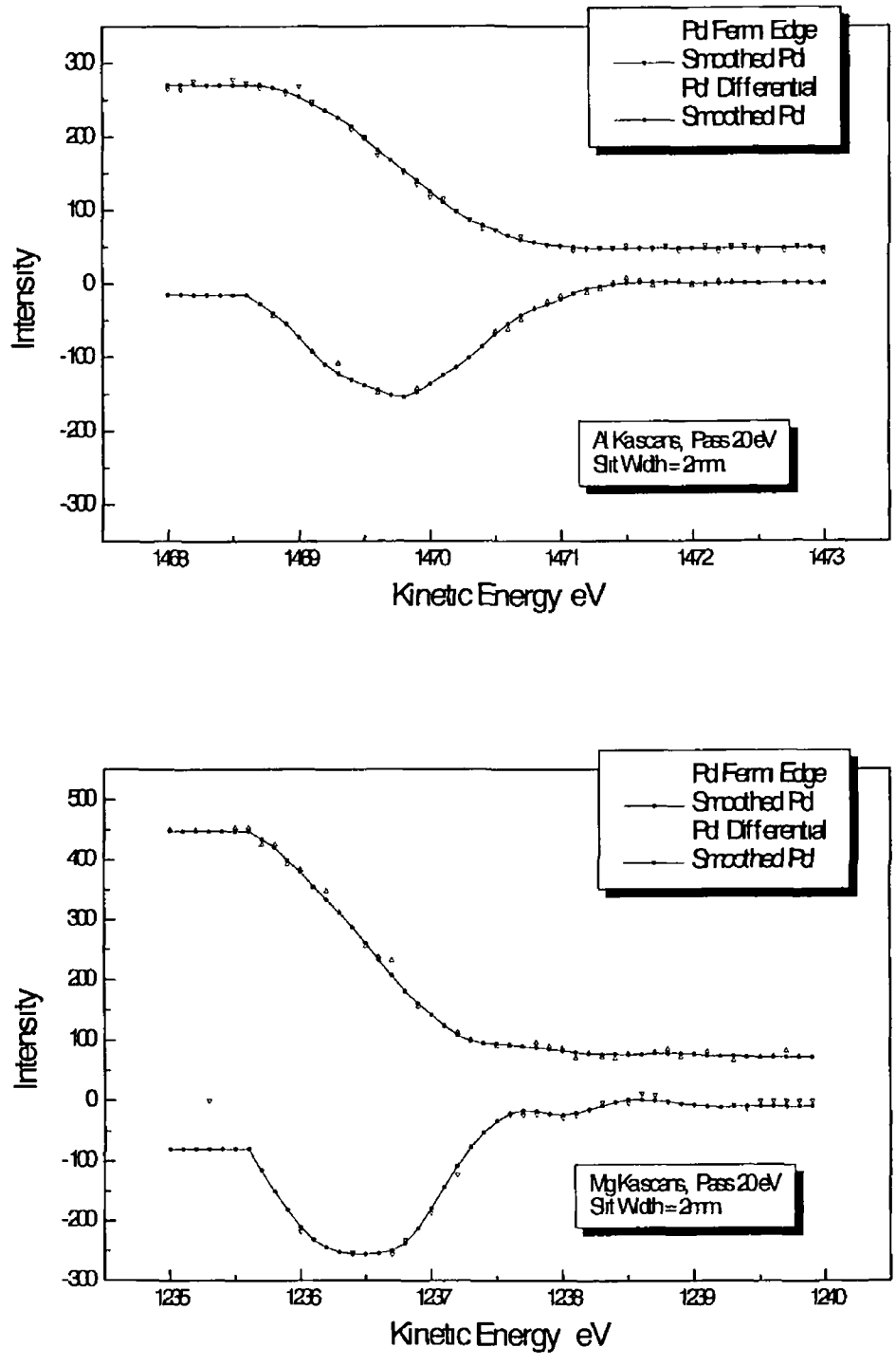

Figure 4.3 · Clam100 Results Typical Pd Fermi edge spectra and the derivative of each Data shown above was taken using the Al Kα x-ray source and below using the Mg Kα x-ray source

Anthony and Seah have shown previously that the data taken with the Mg Kα line are more precise as the narrower line width of this source improves the measurement precision [1] In these studies we have therefore determined the average value of the reference zero with results taken using the MgKα line source only Results as shown in Table 4 2

Spectrometer resolution at the various settings can also be determined from the Fermi edge data This is achieved by noting the energy values at 10% intensity and 90% intensity above the background level, with the difference between these two readings being defined as the resolution, in this case Resolution values for the different spectrometer settings are also listed in Table 4 2 below

X-ray source	**Pass energy eV**	**Slit-Width mm**	**Resolution eV**	**Zero Position eV**
Mg	20	4	1 30	2 2
Mg	50	4	1 44	1 8
Mg	20	2	1 46	1 9
Mg	50	2	1 34	1 9
Mg	20	1	1.51	1 6
Mg	50	1	1 36	1 8
Al	20	4	1 41	1 8
Al	50	4	1 61	1 4
Al	20	2	1 07	1 9
Al	50	2	1 36	1 5
Al	20	1	1 05	2 0
Al	50	1	1 69	1 7

Table 4.2 : Clam100 Results Reference zero positions and resolution data for the Mg Kα and Al Kα sources at various slit widths for 20 and 50 eV pass energies Average values determined from the above results are listed on the following page

Clam100 Energy Calibration Results
Reference Zero (Average) = 1.9 eV ± 0.5 eV.
Resolution (Average) = 1.4 eV ± 0.2 eV.

4.2.2 Clam100 Energy Calibration

Once the reference zero has been defined, the energy calibration can proceed Spectra were taken for cleaned Au, Ag and Cu foil samples using both the Mg Kα & Al Kα sources at pass energies of 20 & 50 eV However, M P Seah cautions that scattering of secondary electrons in the analyser could cause an artificially high background, which would lead to errors in the intensity calibration The problem tends to be worse at low pass energies [4] As can be seen from the spectra shown in Figure 4 4, internal scattering in the Clam100 based spectrometer at a pass energy of 20 eV is much greater than at the 50 eV pass energy level Therefore the energy calibration spectra used were taken at a pass energy of 50 eV The procedure used to carry out the energy scale calibration, using reference energies in conjunction with the spectra taken on the Clam100 spectrometer, is described in Section 4 4 of this chapter

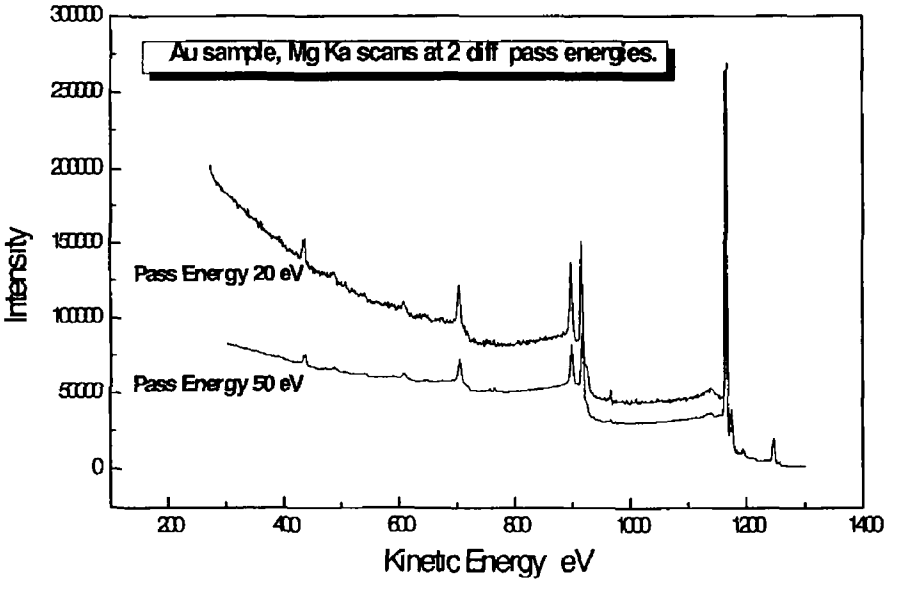

Figure 4 4 : Typical Au spectra showing increased secondary electron scattering at lower pass energies for spectra taken with the VG Clam100 based spectrometer at DCU

4.3 Intensity Calibration

As is the case with energy calibration, the intensity scale must also be calibrated in order to carry out quantitative XPS work In one approach, detailed below, for XPS spectra measured in the pulse counting mode [4], the intensity measured, $I_t(E)$, as a function of the emitted electron energy, E, is given by

$$I_t(E) = I_0 Q(E) n_t(E) \quad (1)$$

where I_0 is the primary x-ray beam flux, Q(E) is the characteristic of the particular instrument for given settings and $n_t(E)$ is the spectrum emitted from sample t Assuming instrumental settings such as pass energy, slit widths, sample position etc are kept constant then Q(E) will be constant and all spectra from that instrument are modified in the same way In practice, all of the parameters cannot be kept constant and so Q(E) may vary to an extent governed by the instrument design

At the National Physics Laboratory (NPL) a *metrology spectrometer,* has been developed in which Q(E) has been characterised for all conditions so that $n_t(E)$ may be deduced for any sample [4] Clearly, if a reference sample can be produced for which $n_t(E)$ is known, this sample can be used in any instrument to calibrate Q(E) via

$$Q(E) \propto I_t(E) / n_t(E) \quad (2)$$

so that that instrument too can generate true spectra, $n_t(E)$

If this is done all instruments should give (1) the same spectrum shape for any given sample, (2) the true spectral shape, $n_t(E)$, traceable to the *metrology spectrometer*

The accuracy with which this can be done depends on (1) the reproducibility of the reference material, (2) the repeatability of the instrument settings, including such parameters as sample positioning and (3) the stability of the instrument components against ageing [4]

It is useful to consider the physical nature of Q(E) Equation (1) may be rewritten

$$I_i(E) = \int_x \int_y \int_{\theta_o} \int_{\phi_o} J_0(x,y) \quad Q(x,y,E,\theta_0,\phi_0) \quad n_i(E,\theta_0)\, dx\, dy\, d\theta_0\, d\phi_0 \qquad (3)$$

where the variations of the x-ray flux density $J_0(x,y)$ over the sample are no longer ignored In Equation (3), x and y are the usual co-ordinate system on the sample surface and θ_0 and ϕ_0 are the photoelectron polar and azimuthal angles of emission For a spectrometer measuring in a particular direction, Equation (3) reduces to

$$I_i(E) = I_0\, n_i(E,\theta_0) \int_x \int_y J_0(x,y) / I_0 \quad Q(x,y,E)\, dx\, dy \qquad (4)$$

We now see that the instrument term Q(E) in Equation (1) is really a result of the integral over the sample surface of the varying x-ray flux density and the electron-optical spectrometer term Q(x,y,E) If the spectrometer term Q(x,y,E) has the same energy dependence for every point x,y on the sample where Q(x,y,E) is non-zero, Q(x,y,E) may be written as the product K(x,y)Q(E) so that

$$I_0 = \int_x \int_y J_0(x,y)\, K(x,y)\, dx\, dy \qquad (5)$$

and Equation (1) is retrieved This means that on a given instrument, use of different x-ray sources with different $J_0(x,y)$ will lead to the same instrument transmission function Q(E) being measured via Equation (2) for all x-ray sources [4] However, for those spectrometers in which the energy and position parts of Q(x,y,E) are not separable, a different curve for Q(E) will be derived via Equation (2) for the different sources

If we consider the simple case [4], where the Q(E) terms are separable, then Q(E) can be written as

$$Q(E) = H(E)T(E)D(E)F(E) \qquad (6)$$

where H(E) is a term describing the aberrations, tolerance and magnetic field distortion contributions to the ideal spectrometer, T(E) is the electron-optical transmission function of the spectrometer, D(E) is the electron multiplier detection efficiency and

F(E) is a term to describe the efficiency of the detector electronics in converting the output to a measured signal For XPS studies spectrometers are usually operated in the constant ΔE mode in which D(E) becomes effectively $D(E_p)$, a constant, where E_p is the spectrometer pass energy Also, as there is little work done at energies below 200 eV where most magnetic field problems occur, H(E) can also be ignored Provided the count rates are not too high and the multiplier voltage and counter discriminator settings are correctly adjusted, F(E) is often unity, which yields

$$Q(E) = T(E) \qquad (7)$$

However, there are 3 specific situations where matters are more complex than the above, they are, (1) with spectrometers in which the area of analysis depends on the energy, (2) spectrometers with a monochromator and (3) spectrometers with internal scattering In the first situation, the Q(E) terms are not separable into spatial and energy terms and this can lead to different calibrations being required for each specific x-ray source Once this situation is identified the separate calibrations are as valid as a single calibration where Q(E) terms are separable [4]

The Clam100 spectrometer at Dublin City University, requires separate calibrations for each x-ray source element As will be seen from the results listed in Section 4.5 of this chapter, the Q(E)-Transmission function curves obtained in this way are similar to other Clam100 curves generated as part of a round robin on intensity calibration carried out previously [4], as shown in Figure 4 5

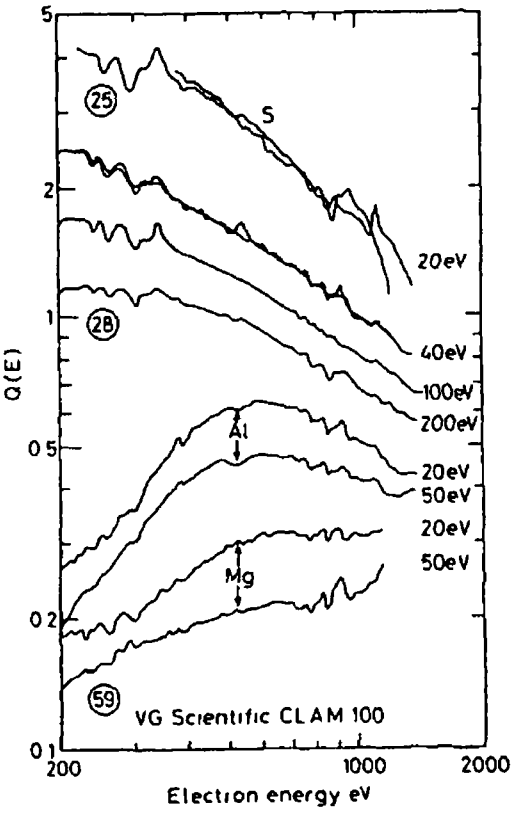

Figure 4.5 Comparison of transmission functions for the VG Scientific manufactured Clam 100 based spectrometer obtained in a previous round robin study [4]

The shortest approach rather than measuring every parameter from first principles is to use reference spectra and divide these spectra into those accumulated on a particular instrument to determine the transmission function of the spectrometer In our studies reference data obtained from VAMAS spectral libraries was used in conjunction with actual spectra obtained to determine Q(E) functions for the Clam100 based system

Once the transmission function spectrum has been accumulated, it can be divided with the VAMAS standard spectra to give a calibration curve This curve can then be divided into any spectrum taken with the same spectrometer to give true quantitative information about the sample being studied

4.4 VAMAS Project

The Vamas project (Versailles project on Advanced Materials and Standards) was set up at the Economic Summit of Versailles in June 1982 One of the working groups organised was the Surface Analysis Society which since 1990 has started projects to construct software to translate spectral data acquired on different machines to the VAMAS-SCA, Standard Data Transfer Format and to construct software to manipulate AES & XPS spectra in a standard manner [5]

The version of the software used here called "The Common Data Processing System" (COMPRO) is Version 3 1, which provides facilities for (1) sharing AES & XPS spectral data, (2) assessing the data processing procedures published in scientific journals and (3) calibrating analysers COMPRO is not a commercial software package but is created by scientists and engineers in the field of surface analysis using electron spectroscopy

The system allows the user to obtain the energy and intensity calibration functions for their particular spectrometer by entering their own spectra which can then be calibrated against standard reference data supplied therein A copy of this software is available from the project leader Dr Kazuhiro YOSHIHARA, National Research Institute for Metals, 1-2-1, Sengen, Tsukaba 305, Japan (e-mail kazuhiro@nrim go jp) [5], [6]

A Energy Scale

The energy scale evaluation is done by referring to the Anthony and Seah calibration data which is listed at the start of this chapter in Table 4 1 For XPS, Cu $2p_{3/2}$, Ag M_4NN, Ag $3d_{5/2}$, Cu L_3MM, Au $4f_{7/2}$ and Cu $3p_{3/2}$ transitions are used as referencing peaks Inputting peak energies for more than three of the above transitions obtained on one's spectrometer, plots the energy dependence of deviations from the reference energies and this can be recorded as an offset function [6]

The offset function has the following form

$$E\ (calibrated) = E\ (observed) + offset\ function,$$

$$where\ offset\ function = X*E + Y$$

For the Clam100 based spectrometer at DCU, offsetting the energy scale by 1 8 eV (Au $4f_{7/2}$ peak) for spectra will give the true peak positions This 1 8eV offset is attributed to an energy/voltage offset in the spectrometer control unit At higher kinetic energies, the offset increased to 3 eV

B. Intensity Scale

The energy dependence of the intensity scale or spectrometer function is defined as follows [6],

$$I(E) = I_s * Q(E) * n(E), \qquad (8)$$

where I_s is the primary beam flux, Q(E) is the spectrometer function, and n(E) is the true distribution of emitted electrons from the sample The intensity scale evaluation is done by referring to the standard spectra data bank in the "Common Data Processing System"

If the spectrometer function of the standard spectra is written as $Q_0(E)$, the standard spectra, $I_0(E)$ is written as

$$Io(E) = I_o * Q_o(E) * n(E) \qquad (9)$$

$$\frac{I(E)/Is}{I_o(E)/I_o} = \frac{Q(E)*n(E)}{Q_o(E)*n(E)} = \frac{Q(E)}{Q_o(E)} = q(E). \quad \textbf{(10)}$$

Therefore, by dividing one's spectrum with the standard spectra, the "relative" spectrometer function or "calibration" function, q(E) can be obtained. [6].

4.5 Clam100 Results : Mg Kα and Al Kα Transmission Functions

Spectra accumulated for the cleaned Gold surface on the Clam100 spectrometer and the corresponding Vamas standard spectra are shown in Figures 4.6 and 4.8, for the Mg Kα and Al Kα sources, respectively. The Clam100 spectra were acquired under the following parameter set.

Parameters	Mg Kα source	Al Kα source
Start Energy (eV)	1252.8	1485.8
Stop Energy (eV)	252.8	485.8
Step Size (eV)	-1	-1
Dwell Time (secs)	1	1
Number of scans	5	5

Table 4.3 : Parameter set used in collection of Clam100 calibration spectra.

The Transmission functions were obtained by dividing the two types of spectra, i.e. the Clam100 spectra and the Vamas standard spectra, to obtain the Transmission function for the x-ray source in question. Figures 4.7 and 4.9, show the Transmission functions for the Mg Kα source and Al Kα source, respectively.

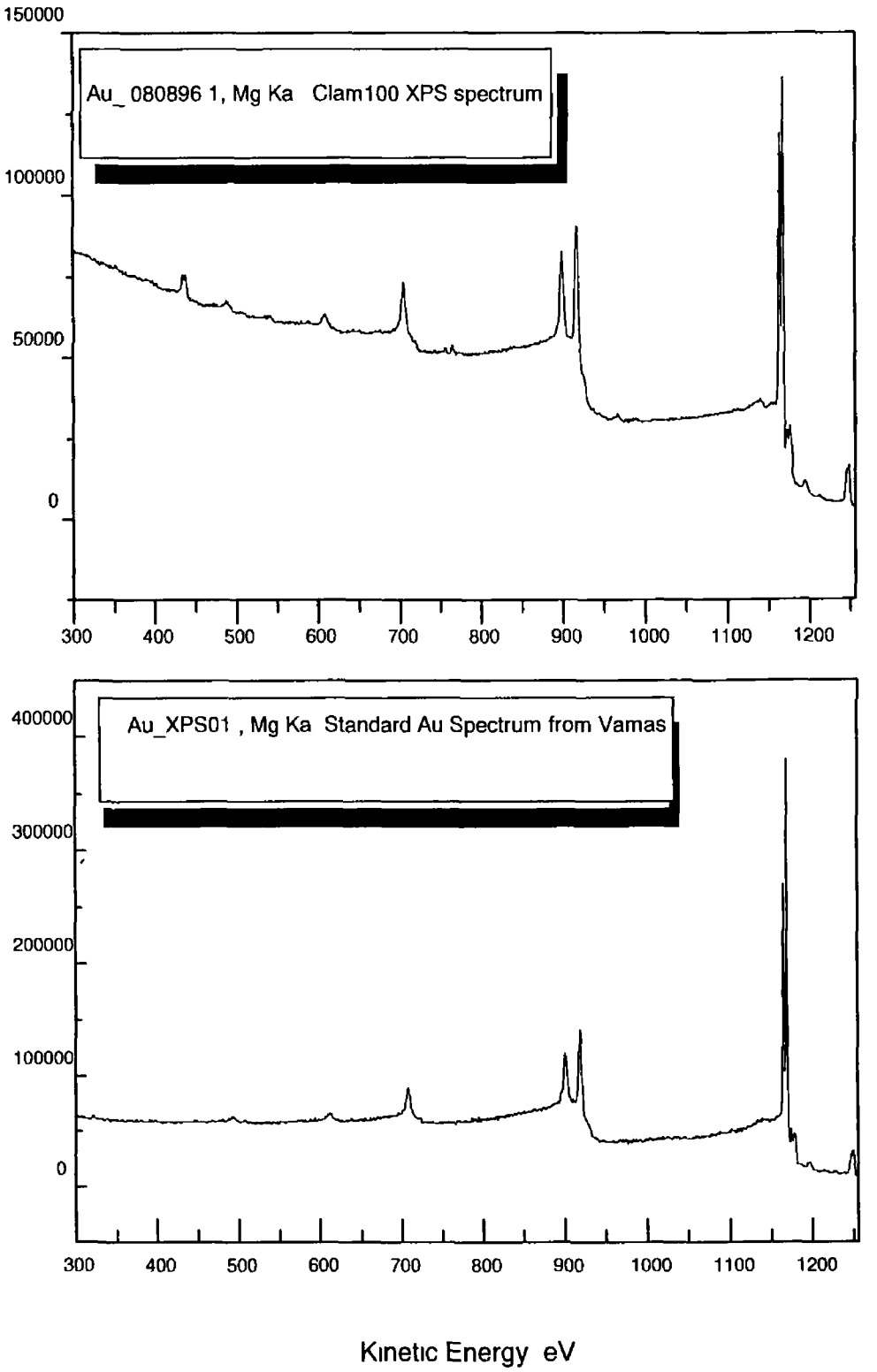

Figure 4 6 · Mg Kα source Spectra used to calibrate the system

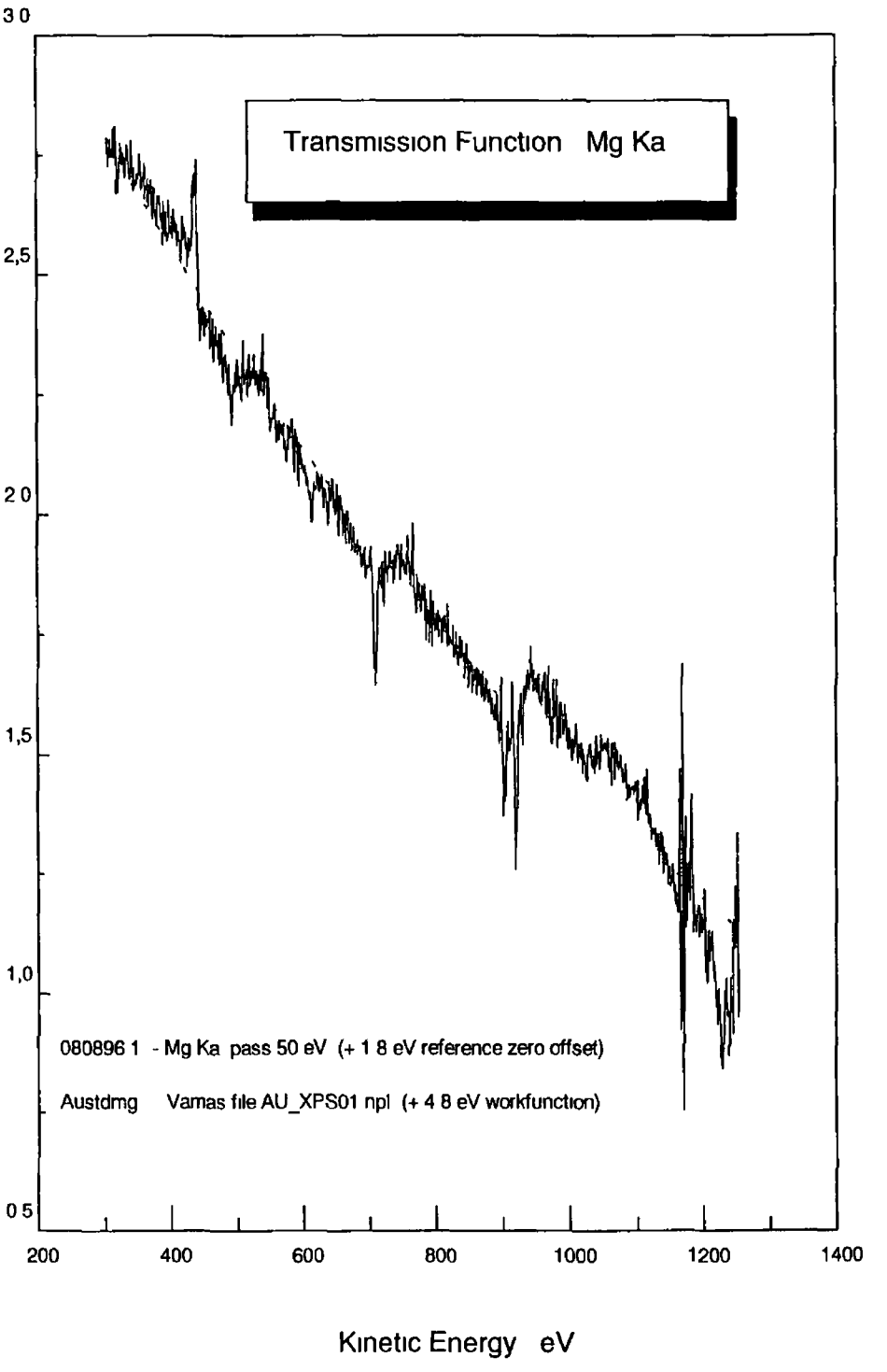

Figure 4 7 : Mg Kα source Transmission Function

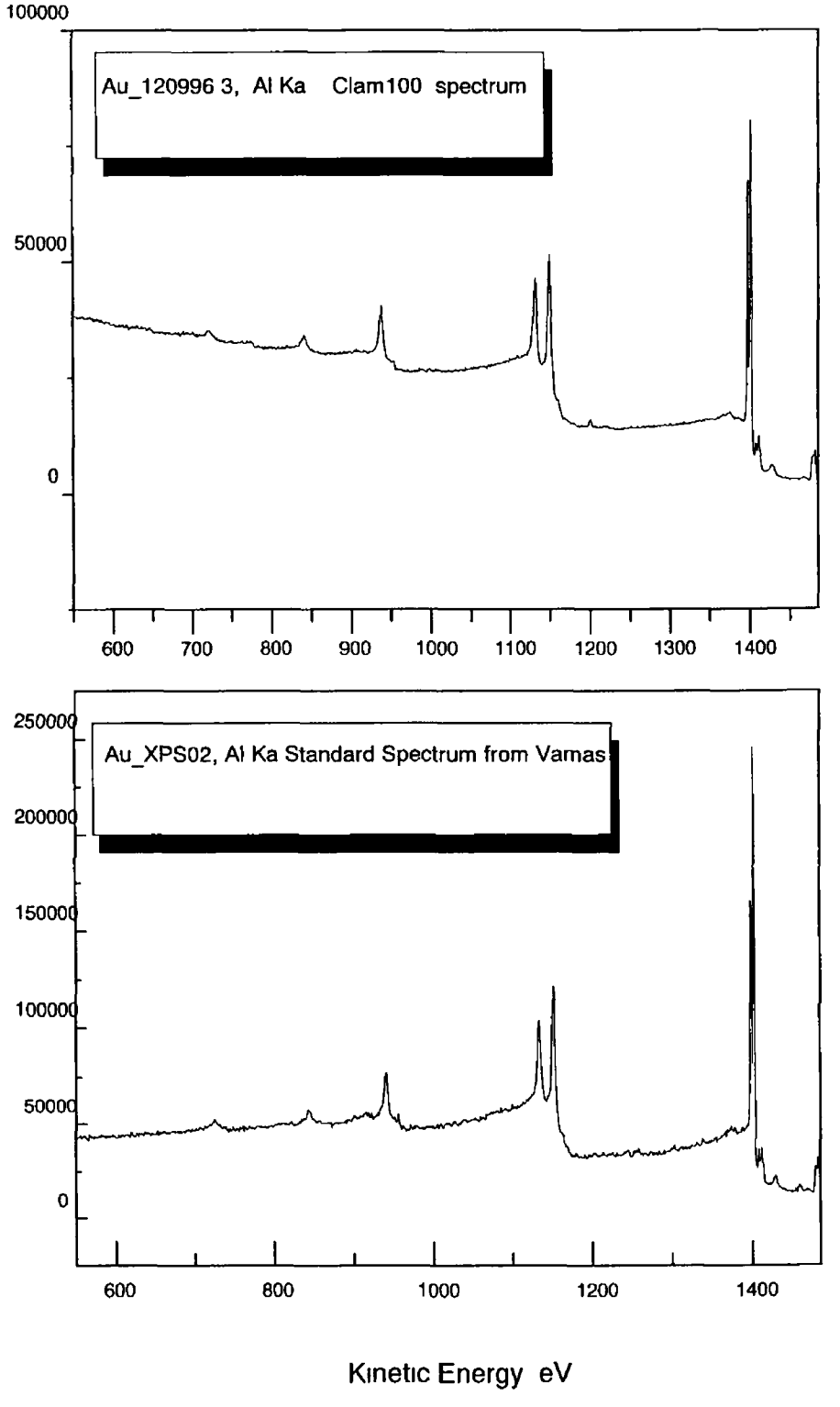

Figure 4.8 : Al Kα source Spectra used to calibrate the system

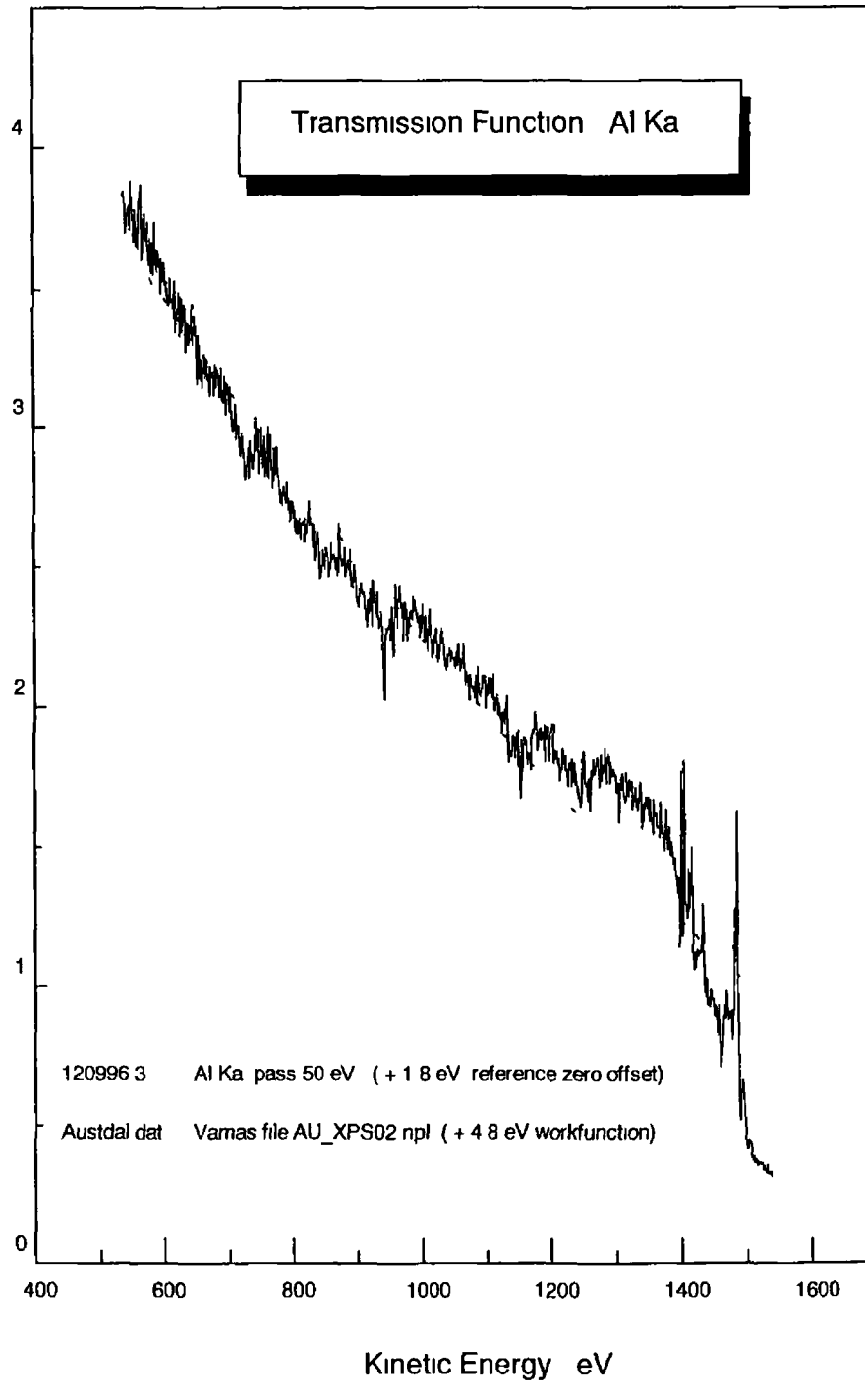

Figure 4 9 : Al Kα source Transmission Function

4.6 E^{-x} Factors

According to Yoshihara and Yoshitake [6], the spectrometer function, Qo(E) of the standard spectra is approximately E^{-1} for XPS Using a more general fit function with a power dependence of E^{-x}, the Clam100, Q(E)'s have the following power dependencies

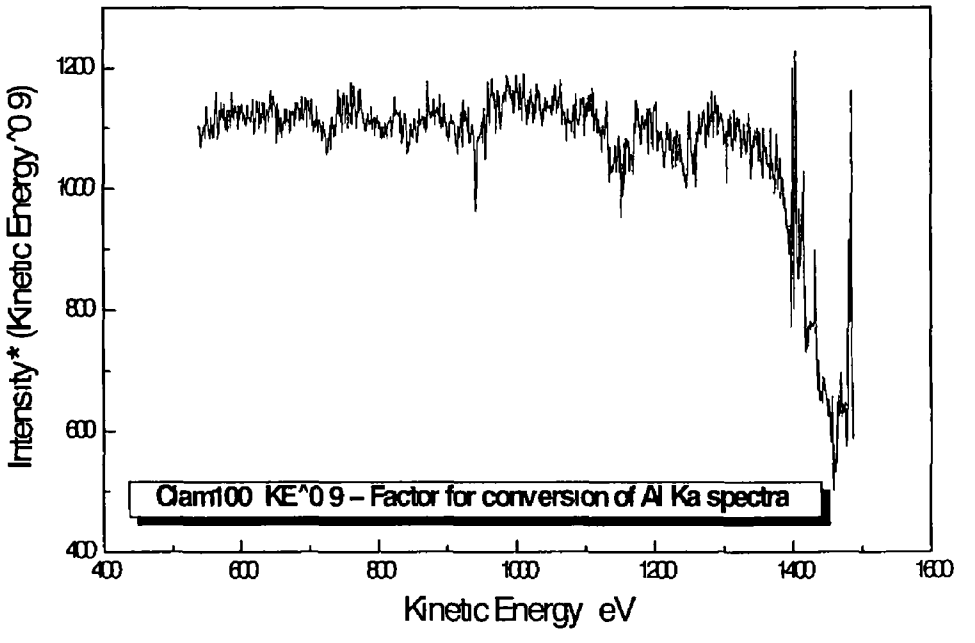

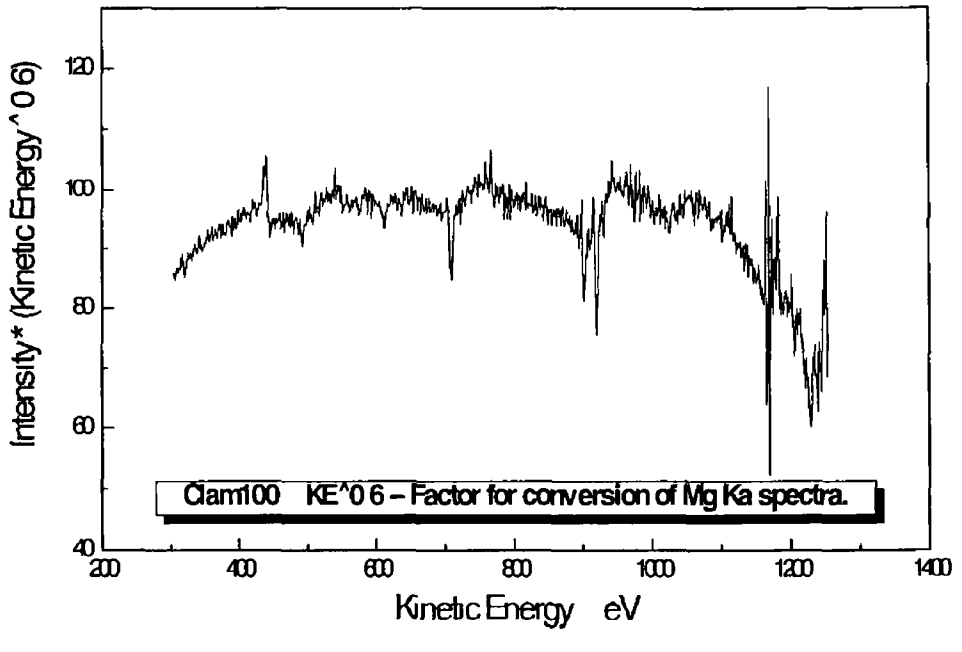

Figure 4.10 : Conversion factors for the Clam100 Mg Kα and Al Kα sources

4.7 Conclusion

Clearly, an accurate and traceable energy and intensity scale calibration must be carried out on each x-ray photoelectron spectrometer that is to be used to carry out quantitative work These calibrations are quite straight forward and once the energy line positions and transmission functions are known for the spectrometer in question, these spectra can then be routinely divided through everyday spectra taken on the instrument Offsetting the spectra taken in this way yields data that can be used to accurately determine elemental concentrations present at the sample surface as well as giving information about the surface bonding environment Spectra taken on regularly calibrated instruments yield results that are meaningful on a wider scale This chapter presents background information on energy and intensity scale calibration and goes on to detail the procedures used to carry out energy and intensity scale calibrations for the Clam100 based spectrometer at the physics department, Dublin City University

4.8 References

[1] M T Anthony and M P Seah, Surface and Interface Analysis, Vol 6, No 3, (1984)

[2] Practical Surface Analysis, Appendix A, Editors D Briggs and M P Seah, Wiley

[3] T L Barr and S Seal, J Vac Sci Technol A, Vol 13, No 3, May/Jun (1995)

[4] M P Seah, Surface and Interface Analysis, Vol 20, 243 - 266, (1993)

[5] VAMAS, Versailles project on Advanced Materials and Standards, The Common Data Processing System, Version 3 1

[6] K Yoshihara and M Yoshitake, J Vac Sci Tech A - Vacuum, Surfaces and Films, Vol 10, Nr 6, (1994)

Chapter 5 Film Thickness Measurements

5.1 Introduction

If XPS is to be used to quantitatively study the thickness of overlayer films on surfaces then the greater the surface sensitivity the better. The major requirement for surface enhancement is that the surface is flat. Clearly, the spectra obtained are strongly dependent on the particular geometry of the XPS system employed., i.e. the relative orientation of x-ray source, sample and spectrometer. With reference to Figure 5.1, if λ is the attenuation length (AL) of the emerging electron then 95% of the signal intensity is derived from a distance 3 λ within the solid. However, the vertical depth sampled is given by

$$d = 3\lambda \mathrm{Sin}\alpha \qquad (1)$$

and this is a maximum when $\alpha = 90^{\circ}$. [1].

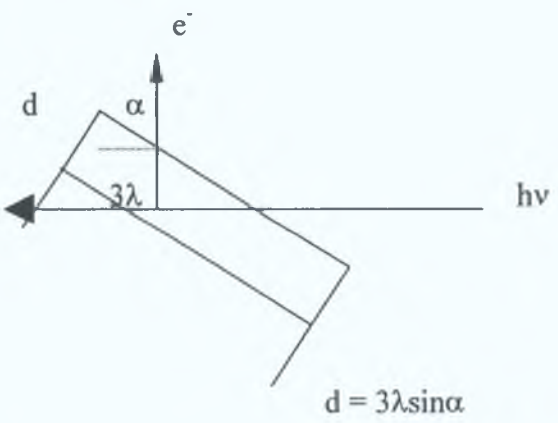

Figure 5.1 : Surface sensitivity enhancement by variation of electron take-off angle.

The E-42 Committee on Surface Analysis of the American Society for Testing and Materials. (ASTM), has composed the following definitions to clarify the most commonly used terms ; with P meaning proposed definition only. [2].

Inelastic Electron Mean Free Path : The average distance (in nanometers) that an electron with a given energy travels between successive inelastic collisions.

Escape Depth : The distance (in nanometers) normal to the surface at which the probability of an electron escaping without significant energy loss due to inelastic scattering processes drops to 1/e (36.8%) of its original value.

P : **Attenuation Length** : The average distance (in nanometers) that an electron with a given energy travels between inelastic collisions as derived from a particular model in which elastic electron scattering is assumed to be insignificant.

P : **Information Depth** : The distance (in nanometers) normal to the surface from which a specified percentage of the detected electrons originates. If the percentage of the electrons detected varies exponentially with distance from the surface, then 63.2%, 86.5%, 95.0%, 98.2% and 99.3% of the detected signal from a homogeneous material originates from within a depth of 1,2,3,4,5 times the electron escape depth, respectively.

Note : The AL is distinguished from the IMFP in that it is derived from a particular type of experiment (the overlayer/film method) and with a particular physical model. [2].

The ED is a direct measure of surface sensitivity for a particular experiment in that it combines the effects of inelastic electron scattering (represented by AL) with the experimental geometry. If photoelectrons are detected by the analyser with some angle θ with respect to the surface normal, the ED will be the AL times Cos θ. Accurate escape depth values are required when using techniques to determine the thickness of thin overlayers on surfaces as discussed in Section 5.3. Several methods of measuring electron escape depths exist. [5].

It is however very difficult to accurately measure electron escape depths and many reviews on the subject exist. [3] & [4]. Unfortunately, markedly different electron escape depths have been measured and published for the same material at the same electron energy, e.g. published silicon data shows a 50% variability.

Also a recent study of electron escape depths in silicon carried out by Hochella and Carim [5], using high resolution transmission electron microscopy (HRTEM) to characterise samples, reports that their escape depths are significantly less than the average of previously published values Electron escape depths measurements for germanium are also quite varied as can be seen in Table 5 1 [6] It is very important to know the correct value of electron escape depth as these values can thereafter be used in formulae to measure oxide film thicknesses

Seah and Dench [1], have developed a set of relationships for different classes of material over the energy range 1 - 6k eV, which approximates the attenuation lengths for many elements and compounds These relationships are listed below

For elements

$$\lambda = 538E^{2} + 0\,41(aE)^{0.5} \text{ monolayers} \quad [1\,36]$$

For inorganic compounds

$$\lambda = 2170E^{-2} + 0\,72(aE)^{0.5} \text{ monolayers} \quad [1\,38]$$

For organic compounds

$$\lambda = 49E^{2} + 0\,11E^{0.5} \text{ mg/m}^{2} \quad [2\,10]$$

where a is the atom size (in nm`s) and E is the electron energy (in eV`s) The number in the square brackets represents the factor of one standard deviation uncertainty describing the scatter of the data

More recently Tanuma, Powell and Penn [7], [8] have derived theoretical inelastic mean free paths (IMFP's) for 27 elements and 4 compounds, for $50 \leq E \leq 2000$ eV

5.2 λ (E) Literature Values for Germanium

Material Amorphous	Electron line	Photon	Electron energy eV	λ(E) nanometers	References
Ge	Au $4f_{7/2}$	Al Kα	1404	2.9 ± 0.4	1
Ge	Au $4f_{5/2}$	Al Kα	1400	2.9 ± 0.4	1
Ge	Au $4d_{5/2}$	Al Kα	1153	2.5 ± 0.3	1
Ge	Ge $L_3M_{4,5}M_{4,5}$	Al Kα	1137	2.6 ± 0.3	1
Ge	Ag $3d_{5/2}$	Al Kα	1121	2.3 ± 0.3	1
Ge	Ag $3d_{3/2}$	Al Kα	1114	2.2 ± 0.3	1
Ge	Cu $L_3M_{4,5}M_{4,5}$	Al Kα	920	2.2 ± 0.3	1
Ge	Cu 2p 3/2	Al Kα	554	1.7 ± 0.2	1
Ge	Ag $M_4N_{4,5}N_{4,5}$	Al Kα	355	1.2 ± 0.1	1
Ge	Ag $M_4N_{4,5}N_{4,5}$	Al Kα	350	1.2 ± 0.1	1
Ge	Cu 3p	Al Kα	203	0.89 ± 0.06	1
Ge	Au 4f	C Kα	192	0.86 ± 0.06	1
Ge	Au Auger	C Kα	73	1.1 ± 0.1	1
GeO_2	Various	Al Kα	234	0.61	2
GeO_2	Various	Al Kα	266	0.68	2
Crystalline					
Ge	Auger	Electrons	1147	2.31 ± 0.2	3
Ge	Auger	Electrons	25-130	< 0.7	3
Ge	*Theoretical*	*Work*	1000	1.51	4

Table 5.1 : Table of previously published λ(E) values for Germanium, including oxides.

5.3.1 Methods of determining oxide film thicknesses

Several well-known film thickness measurement techniques exist [5] & [9] They are used mainly in the determination of SiO_2 film thicknesses but are equally as valid for the determination of GeO_x film thickness According to Hochella and Carim [5], the simplest way to measure the thickness of an overlayer film is to, measure the intensity of a peak originating from the film I_f, which should increase with the film thickness according to the relationship

$$I_{f,x} = I_{f,\infty} (1 - e^{-x/(\lambda f \, Sin \, \theta)}) \qquad (1)$$

where $I_{f,x}$ is the intensity of an oxide peak from a film of thickness x, $I_{f,\infty}$ is the corresponding peak from an infinitely thick film and λ_f is the AL for the film in question with θ being the take-off angle, and where $\theta = 90°$ is normal to the surface

Conversely, one could also measure the intensity of a peak originating in the substrate, which should decrease exponentially with overlying film thickness according to

$$I_{s,x} = I_{s,o} \, e^{-x/(\lambda f \, Sin \, \theta)} \qquad (2)$$

where $I_{s,x}$ is the intensity of the substrate peak using a sample covered with a film of thickness x and $I_{s,o}$ is the corresponding peak from an oxide-free (hydrogen passivated) substrate They state two disadvantages to these techniques (and for any technique requiring the measurement of intensities from two or more different samples) as follows, that very stable and reproducible analysis conditions are required and that the data will require a sizeable correction for any overlayer of adventitious carbon, which will differ for each sample

Several authors are in agreement that the best solution is to base the analysis on the ratio of a substrate peak and oxide peak separated only by the chemical shift This technique is known as the Ratio method and is not described here but is detailed in Chapter 6, where it is used to calculate the thickness of the oxide overlayer on several Ge samples

5.3.2 Curve fitting

In order to use the techniques given above the intensities of the peaks in question must be accurately known This is normally achieved through the curve-fitting of the XPS spectral data obtained All the peaks required can be characterised under parameters such as peak position in eV, peak intensity and Gaussian and Lorentzian line broadening and the inelastic background can also be subtracted from the spectra An iterative least squares fitting program called "bfit" was used throughout the work reported here [10] Parameters are listed in chapter 6, Table 6 1

5.4 Native Oxide on Germanium : Clam100 Results

Using the method described in section 5 3 1 above and the peak intensity estimations determined by curve fitting the peaks in question, namely the Ge peak and the GeO_x peak, it is possible to reproducibly calculate the thicknesses of the native oxides on untreated germanium surfaces Native oxide thicknesses were determined for both the Ge(111) and Ge(100) surfaces Examples of some thicknesses calculated are given in Table 5 2 below

Samples All surfaces untreated	Native Oxide thickness in nm's
Ge (111) surface	1 6
Ge (100) surface	1 8
Ge (100) surface	1 8

Table 5.2 Clam100 Results Native oxide thicknesses on untreated Ge surfaces

These results are in agreement with previously reported native oxides on silicon surfaces, which are generally about 2 nm's in thickness An accurate measurement of the thickness of the native oxide on germanium is a necessary starting point from which to advance to further studies on methods of removal of this native oxide layer

5.5 Conclusion

With reference to Table 5 1, the importance of selecting the attenuation length corresponding to the energy position of the actual peaks you are working with as opposed to a general value for the material in question, can be seen Several methods of calculating film thicknesses also exist with each method having its own advantages and drawbacks attached Once the correct attenuation length and overlayer thickness measurement technique have been selected for the study required, an accurate and repeatable native oxide thickness for each untreated sample can easily be determined

5.6 References

[1] Practical Surface Analysis, Vol 1, Editors D Briggs and M P Seah (Wiley)

[2] C J Powell, J of Electron Spectro and Relat Phenom 47 (1988) 197-214

[3] M P Seah and W.A Dench, Surface Interface Analysis, (1979), 1

[4] C.J Powell, Scanning Electron Microscopy, 1984 / IV, Ed O Johari

[5] M F Hochella and A H Carim, Surface Science, 197 (1988) L260-L268

[6] J Szajman, J G Jenkins, J Liesegang and R C G Leckey, J of Electron Spect and Relat Phenom 14 (1978) 41-48, and references therein, excluding crystalline Ge data

[7] S Tanuma, C J Powell and D R Penn, Surf Interface Anal , 12, 87 (1988)

[8] S Tanuma, C.J Powell and D R Penn, Surf Sci 192, L849 (1987)

[9] D F Mitchell, K B Clark, J A Bardwell, W N Lennard, G R Massoumi, I V Mitchell, Surface and Interface Analysis, Vol 21, 44-50, (1994)

[10] Unpublished Bfit is a curve-fitting program developed by Wolfgang Theis and Andreas Hempelmann, University of Berlin , Germany

References from Table 5.1

[1] J Szajman, J G Jenkins, J Liesegang and R C G Leckey, J of Electron Spect and Relat Phenom 14 (1978) 41-48

[2] C.J Todd and R Heckingbottom, Phys Lett 42A (1973) 455

[3] H Gant and W Moench, Surface Science 105 (1981) 217-224

[4] References contained in [3] above, namely [3] (C.J Powell) and [6] (M P Seah and W A Dench) therein

Chapter 6: An x-ray photoelectron spectroscopy study of the HF etching of native oxides on Ge (111) and Ge (100) surfaces

6.1 Introduction

In this chapter an x-ray photoelectron spectroscopy (XPS) study of the removal of the native oxides from the Ge (111) and Ge (100) surfaces by hydrofluoric (HF) acid based etch treatments is presnted A range of different etch procedures were investigated A cyclic HF etch, water rmse procedure which was repeated a number of times before loading the samples into the XPS chamber was found to be an effective surface oxide removal treatment This procedure is compared with the removal of the native oxide by in-situ argon ion bombardment In the analysis, Germanium 2p and 3d core level data was collected together with C 1s and O 1s data The Ge 2p and 3d core levels have a wide kinetic energy separation of significantly different escape depths By consistently curve fitting the chemically shifted oxide peaks for these two core levels it was possible to determine the thickness of the residual oxide coverage on the chemically etched surfaces Rates of native oxide re-growth as a function of exposure to ambient conditions were also monitored These oxide regrowth rates were found to be comparable to those reported for hydrogen passivated silicon surfaces suggesting that the chemical procedures used on germanium resulted in the formation of hydrogen terminated surfaces

A major technological drawback to the utilisation of germanium in mainstream device fabrication has been the difficulty in growing an insulating oxide comparable to SiO_2 in silicon technology Indeed, while the oxidation of silicon has been extensively investigated by a wide range of techniques, there are relatively few photoemission studies of germanium oxidation [1-5] These studies have highlighted the differences in the oxidation chemistry of the two elements despite their identical bulk structures and proximity in the periodic table In addition, there have been even fewer papers [6,7] which have addressed the important process of native oxide removal which is a necessary preparation step to heterostructure growth From a technological viewpoint, the fact that Ge has a narrower bandgap than Si and has high hole mobility makes it a

potential candidate for high performance device applications [8] In addition, the increase in the number of research investigations of Ge/Si alloy materials necessitates an understanding of the oxidation of these materials, a process which is critical in silicon device fabrication In this thesis, we present the results of an effective HF based treatment designed to remove the native oxides from Ge(111) and Ge(100) surfaces and a study of the rate of oxide regrowth on these surfaces under ambient conditions It is well known in the literature that HF based treatments of the low index faces of silicon result in the removal of the native oxides and the termination of the surface dangling bonds with hydrogen These hydrogen passivated surfaces are resistant to ambient oxidation This study sets out to determine whether a similar passivating effect is observed on germanium

6.2 Etch procedures

Initially a H_2O_2 based treatment was used to grow a thin oxide layer on the sample surface Several atomic layers of Ge were then removed using a HF etch/water rinse procedure [7] The next etch procedure tried, involved following the last step above by heating the sample in di-iomsed water for several minutes (usually 5-10 mins) at 60 / 70 ^{o} C before insertion into vacuum The reason for this heating step is that GeO_2 is known to be water soluble [4] The peroxide (H_2O_2) growth stage was then removed from the treatment, with samples being dipped in dilute HF for 15 secs, rinsed in di-ionised (DI) water and the procedure repeated from 3-5 times before drying the sample in N_2 gas and insertion into the vacuum system Examples of the Ge 3d spectra obtained by these etch procedures are shown in Figure 6 1 below It is clear that the thickness of the oxide layer has been significantly reduced, however, they have not succeeded in producing a clean oxide free surface

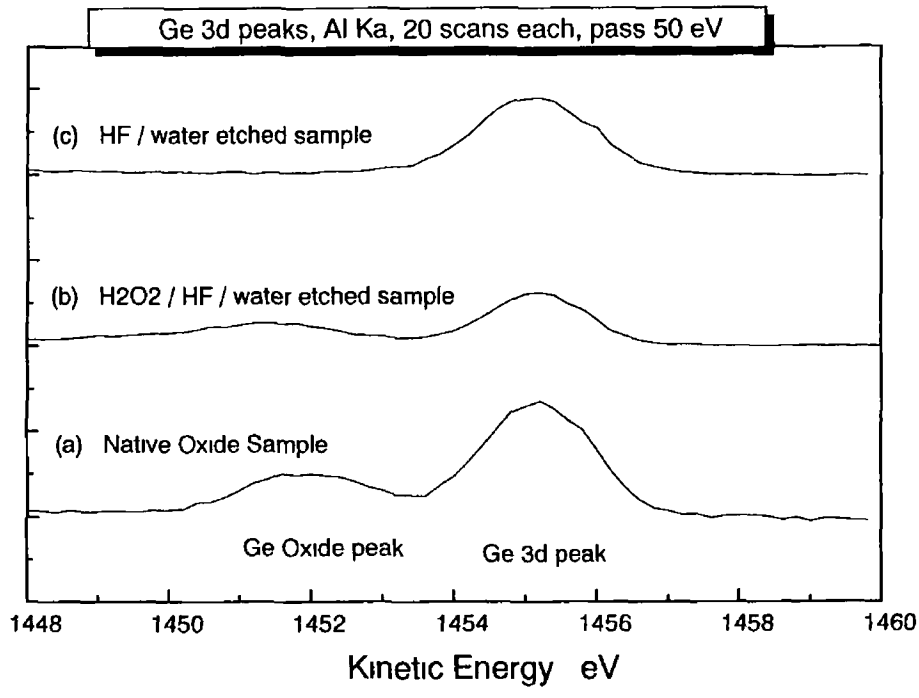

Figure 6 1 Ge 3d data Chemical etches, (a) Native Oxide sample for comparison with, (b) H_2O_2 / HF / water etched sample and (c) HF / water etched sample

Another treatment investigated included, a repetition of the HF-based cleaning procedure with the last step being a 2 min etch in NH_4F at room temperature before final DI water rinse This procedure was tried because it is known that for silicon, the use of an NH_4F etch produces a very flat hydrogen terminated surface Finally a HF-based cleaning procedure as above with final steps following the last HF etch involving, heating the sample in an aqueous $(NH_4)_2S_X$ solution (10 ml $(NH_4)_2S_X$ in 50 ml DI water) for 10 mins at 60° C, followed with a room temperature dip in an second aqueous $(NH_4)_2S_X$ solution (1 5) for 2/3 secs was carried out, the sample was then rinsed in methanol and dried in N_2 gas [9] The reason for this last treatment was to determine whether it was possible to sulphur terminate the Ge surface using wet chemical procedures, however this work was never pursued

6.3 Experimental

Ge (111) and Ge (100) single crystal samples were studied using XPS with measurements being made in a VG Clam 100 spectrometer, with a twin anode X-ray source. Al Kα and Mg Kα radiation lines were employed, with either source being operated at an anode voltage of 15 kV with an emission current of 20 mA. The analyser pass energy was 50 eV with a step size 0.2 eV and a dwell time of 1 sec.

In the experiment, Ge 2p and Ge 3d peak data was collected together with carbon 1s and oxygen 1s peak data. Data was collected from the native oxide untreated surface and HF etched samples. The HF treated samples were then removed from the vacuum chamber and left in air for periods of time up to one month before re-examination. Several different Ge samples were used to check reproducibility.

It was found that the most effective method of removing the native oxide layer was a cyclical HF/water rinse etch. Samples were rinsed in running water (purified to < 100 ppm) for approximately 20 seconds, dipped in HF acid (50% solution : LSI 1 class) for 10 seconds and water rinsed again. This procedure was repeated a total of 5 times before drying the sample in filtered N_2 gas and then immediately inserting it into a fast entry load lock connected to the spectrometer.

6.4 Results

Typical Ge 3d and $2p_{3/2}$ spectra for the (111) surface obtained are shown in Figures 6.2 and 6.3. Spectra for the (100) surface are shown in Figures 6.4 and 6.5. The kinetic energies of the Ge peaks originating from the substrate correspond to previously observed binding energy values. [4]. The peaks at lower kinetic energy i.e. higher binding energies correspond to Ge in its oxidation states GeO_x ($x \leq 2$). Chemical shifts of approximately 3 eV for the Ge $2p_{3/2}$ and Ge 3d data correspond to the typical eV separation values of GeO_2 [4]. Large amounts of carbon and oxygen were visible on the surface of all untreated Ge samples. These signals originate from a combination of adventitious carbon, hydrocarbon and water absorbed onto the surface during its exposure to ambient conditions since manufacture.

Figure 6.2 shows the Ge 3d spectra for the Ge(111) surface before and after HF etch treatment. A curve fitting routine was used to identify the component peaks of the spectra, with parameters as shown in Table 6.1 below. (background removal not shown). The native oxide spectrum required a two peak fit indicating that the native oxide was primarily GeO_2. This oxide component peak completely disappeared following the described HF etching procedure. The oxygen 1s peak was also no longer visible following the HF etch, while a small carbon 1s signal was always present. Even after a week's exposure to ambient laboratory conditions the native oxide component is hardly visible in the spectrum. The spectra for the Ge $2p_{3/2}$ shown in Figure 6.3 are much more sensitive to changes in the surface composition because of the significantly reduced mean free path for electrons with low kinetic energies. The real effectiveness of the HF etch treatment is apparent in these spectra as the $2p_{3/2}$ can be fitted with a single peak indicating the total removal of the native oxide within the detection limits of the technique. The re-oxidation of the etched surface can also be more clearly seen after air exposure. The Ge 3d and 2p spectra for the Ge(100) surface before and after HF etch treatment exhibited the same general trends as observed for the Ge(111), as shown in Figures 6.4 and 6.5 below.

Etched Ge surface parameters		Oxidised Ge surface parameters	
Inte1	Ge peak intensity	*Inte 1/2*	Ge & Oxide peak intensities
Peak 1	Ge peak position	*Peak 1/2*	Ge & Oxide peak positions
Gamm 1	Ge peak Lorentzian broadeng	*Gamm 1*	Ge & Oxide peak Lorentzian
Broa 1	Ge peak Gaussian broadening	*Broa 1*	Ge & Oxide peak Gaussian
Typical values : *2p peak*	1.98 ± 0.02 eV	*Oxide peak*	2.32 ± 0.07 eV
3d peak	1.52 ± 0.06 eV	*Oxide peak*	2.27 ± 0.10 eV

Table 6.1 : Curve fitting parameters used for Ge 3d & 2p substrate and oxide peaks.

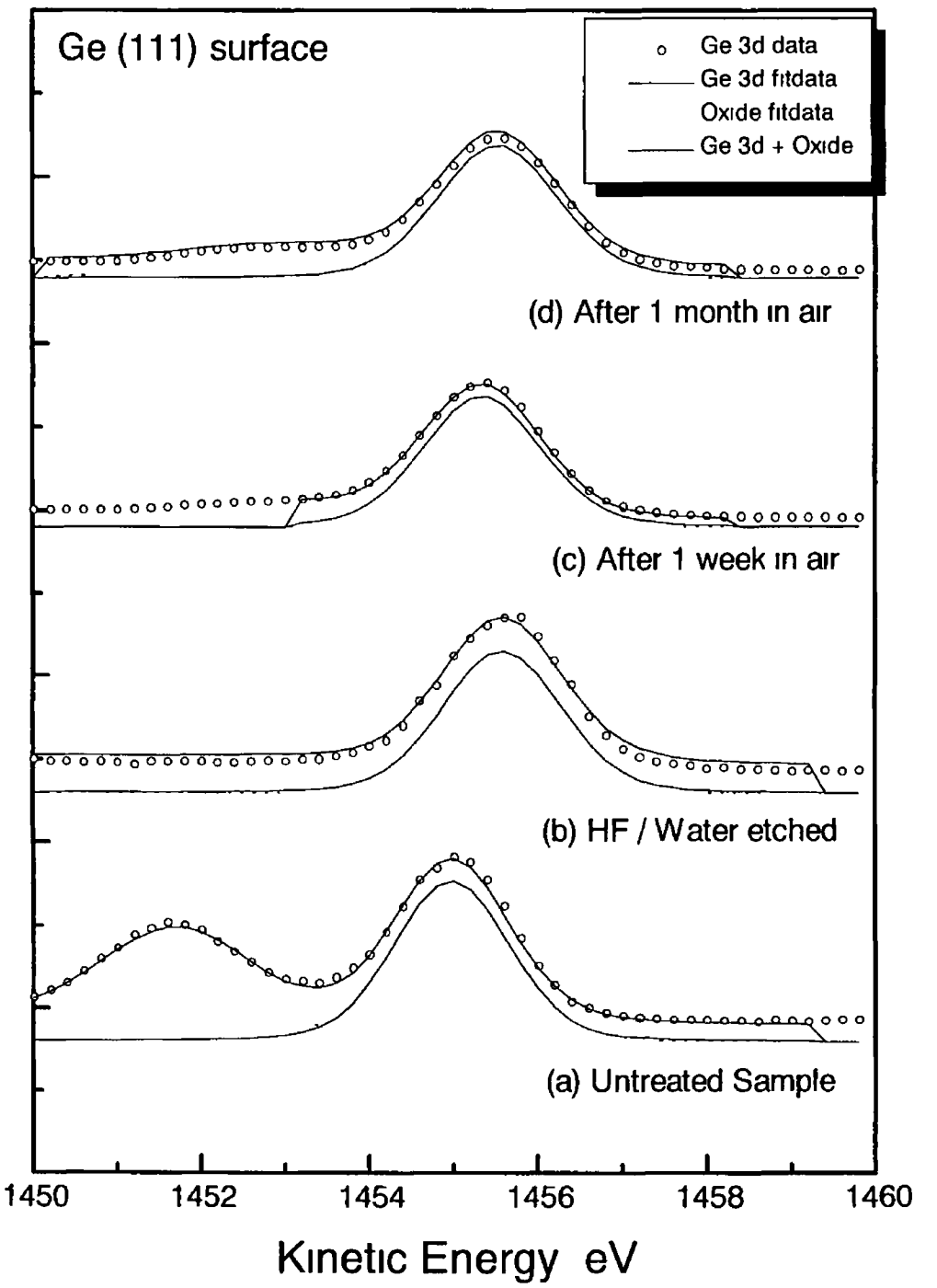

Figure 6.2 Ge (111) data Typical Ge 3d spectra (a) untreated, (b) HF/water etched, (c) etched samples after 1 week in air and (d) etched samples after 1 month in air

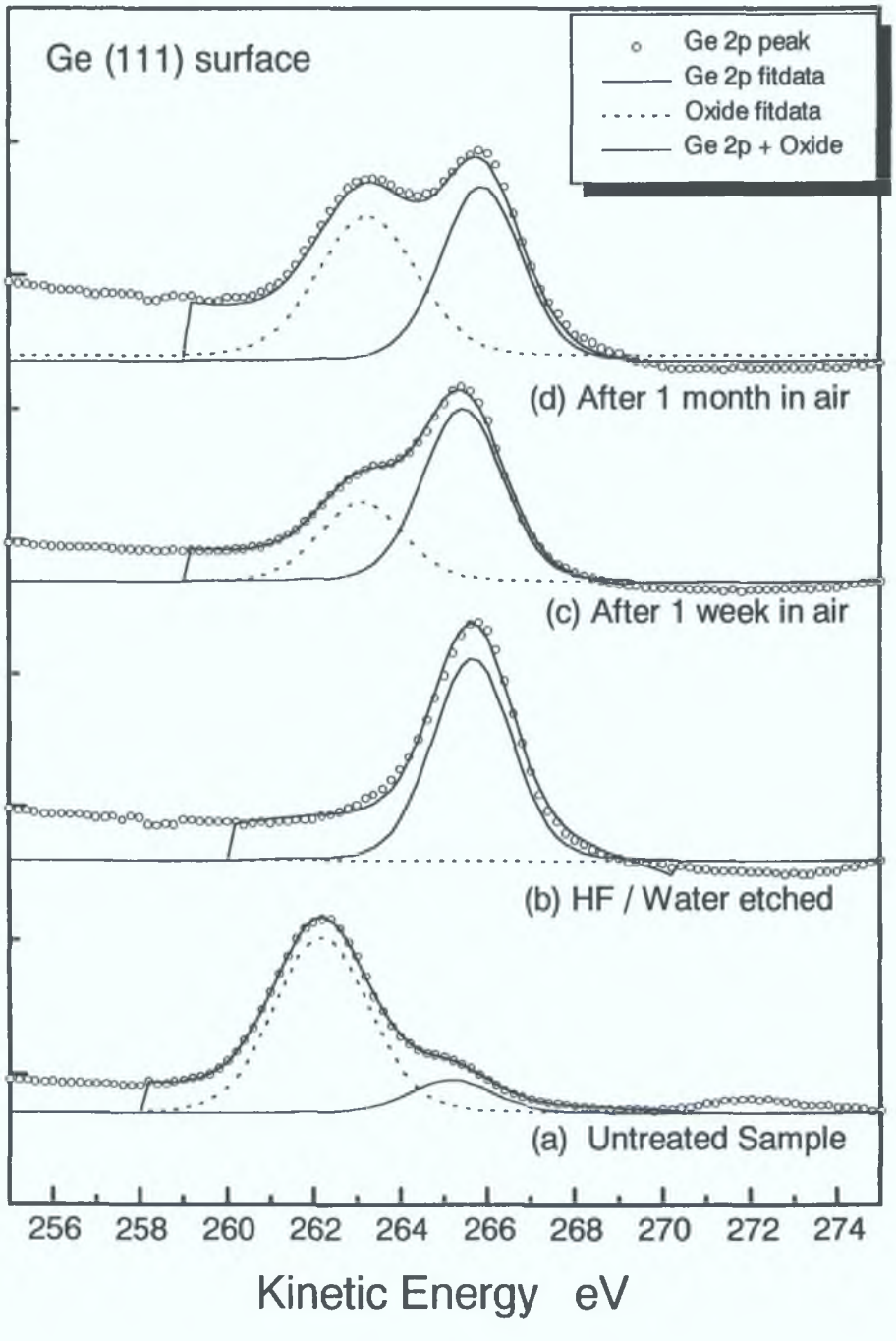

Figure 6.3 : Ge (111) data : Typical Ge $2p_{3/2}$ spectra. (a) untreated, (b) HF/water etched (c) etched samples after 1 week in air and (d) etched samples after 1 month in air.

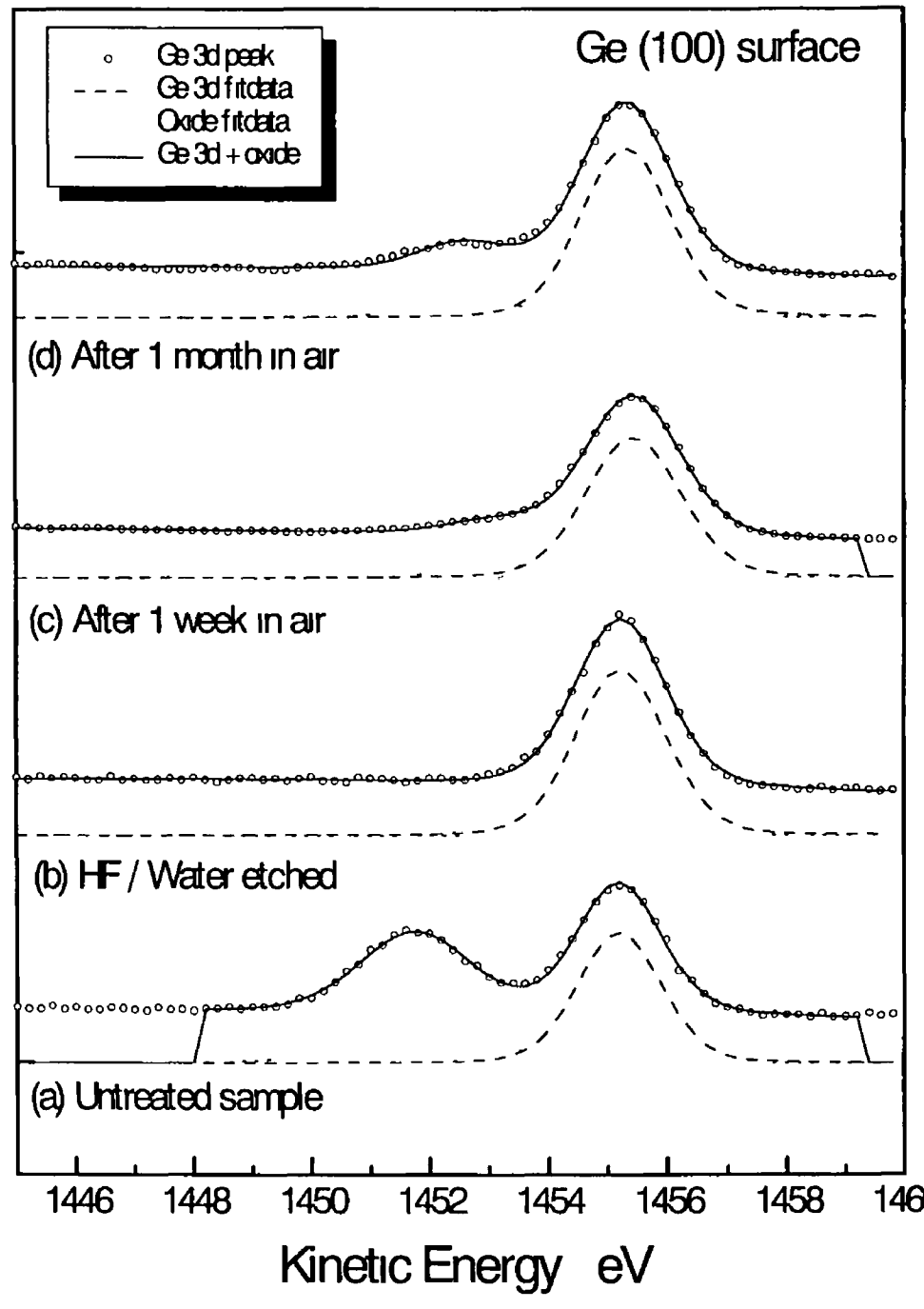

Figure 6 4 Ge (100) data Typical Ge 3d spectra (a) untreated, (b) HF/water etched, (c) etched samples after 1 week in air and (d) etched samples after 1 month in air

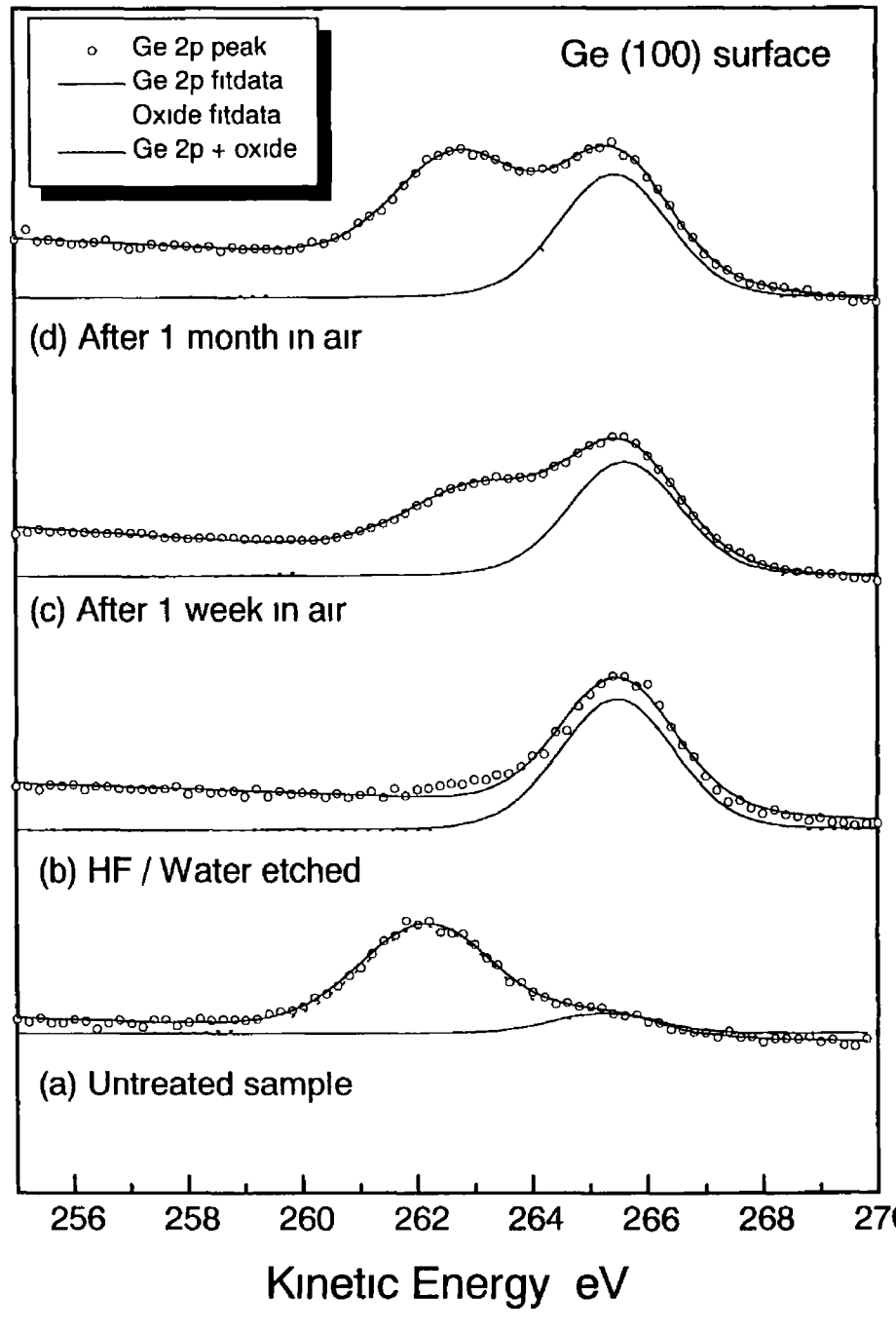

Figure 6.5 Ge (100) data Typical Ge $2p_{3/2}$ spectra (a) untreated, (b) HF/water etched (c) etched samples after 1 week in air and (d) etched samples after 1 month in air

6.5 Argon Ion bombardment

Another method of removing the native oxide from a surface is by in-situ argon ion bombardment. (see chapter 3). In this experiment samples were bombarded using this method until no oxygen 1s peak was visible in the XPS spectrum. Samples were then removed from the vacuum chamber and left to reoxidize under ambient conditions while monitoring re-growth rates. Figure 2 below shows the differences between the two methods. Clearly, there is a much faster oxide re-growth rate for the argon bombarded samples suggesting that the chemical HF/water rinse treatment is much more effective as an oxide re-growth suppressant. (It is known that argon ion sputtering can generate surface defects, which can be minimised by a moderate temperature anneal which none the less introduces another preparation stage into the cleaning process. [7 referenced therein 4,5,6].)

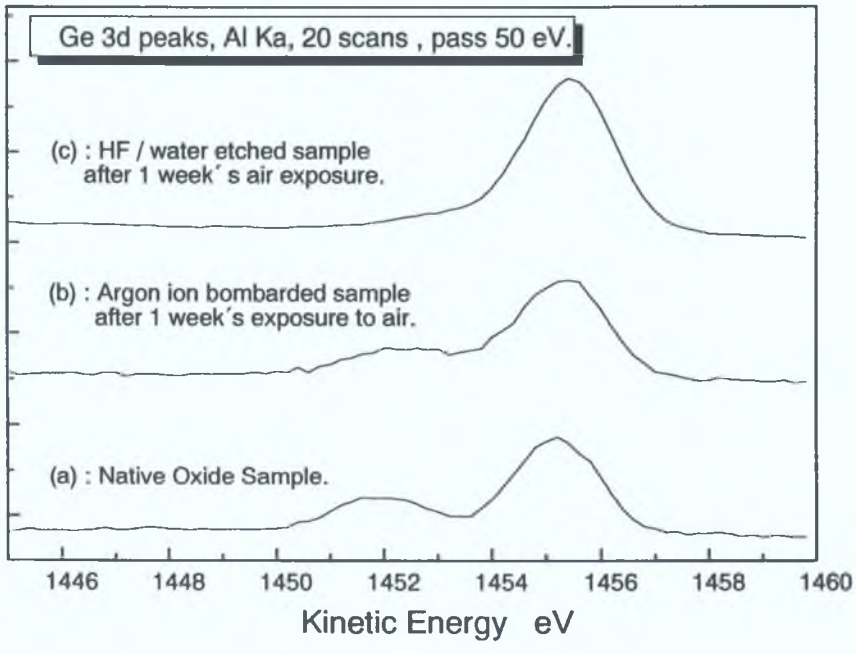

Figure 6.6 : Ge 3d peak data : Oxide regrowth (a) Native Oxide sample for comparison with (b) in-situ argon ion bombarded Ge sample, and (c) HF / water etched Ge sample, following 1 week's exposure to air.

6.6 Overlayer thickness estimation

The thickness of the overlayer present on the native oxide samples and the HF etched samples left in air was estimated from the comparison of the intensity ratios of substrate ($I_{s,x}$) and oxide ($I_{f,x}$) peaks for the Ge 3d and Ge $2p_{3/2}$ core levels which have significantly different sampling depths. This method is appropriate when the same element exists in two distinct chemical environments, elemental Ge and oxidised GeO_2. The thickness of the native oxide overlayer x, is calculated from

$$x = \lambda_f \, Cos\, \theta \, ln(1 + 1/Q) \qquad (1)$$

where

$$Q = (I_{s,x}/I_{f,x}) \, . \, (I_{f,\infty} /I_{s,o}) \qquad (2)$$

λ_f is the attenuation length and θ is the angle between surface normal and the emission direction (15° in this case). For a sample covered with a film of thickness x, the ratio of the intensity of the photoemission peaks from the substrate and the oxide is $I_{s,x}/I_{f,x}$. This method requires two absolute intensities in order to measure $I_{f,\infty}/I_{s,o}$, which is the ratio of the intensities of the photoemission core level peaks for an infinitely thick oxide sample to that of the substrate peak for an oxide-free sample. Once this ratio is known, $I_{s,x}/I_{f,x}$ can be measured for various oxide thicknesses with the advantage that effects of slight variations in analysis conditions, e.g. sample alignment are minimised. The advantage in using two photoemission peaks, Ge $2p_{3/2}$ and Ge 3d, is that by taking the ratio of $I_{s,x}/I_{f,x}$ for the two sets of spectra, the absolute intensity ratio $I_{f,\infty}/I_{s,o}$ is common and therefore cancels out. For this approach, we have taken the average of previously published experimentally determined escape depth values of Szajman et al.[11] and Gant and Monch [12] for the Ge $2p_{3/2}$ and Ge 3d subshells, which are 0.9 ± 0.1 nm and 3.0 ± 0.3 nm, respectively. Overlayer thickness estimates using these λ_f values and ratio method calculations are shown in Figures 6.7 and 6.8, for two different HF etched Ge(111) and Ge(100) samples respectively, with an untreated (native oxide) sample included for reference purposes. Typically native oxide thicknesses were in the range 2 - 3 nm which is comparable to the values reported for silicon [10]. The consistency of the oxide regrowth rates can be deduced from the fact that the graphs include two different samples for both the Ge (111) and Ge (100) surfaces.

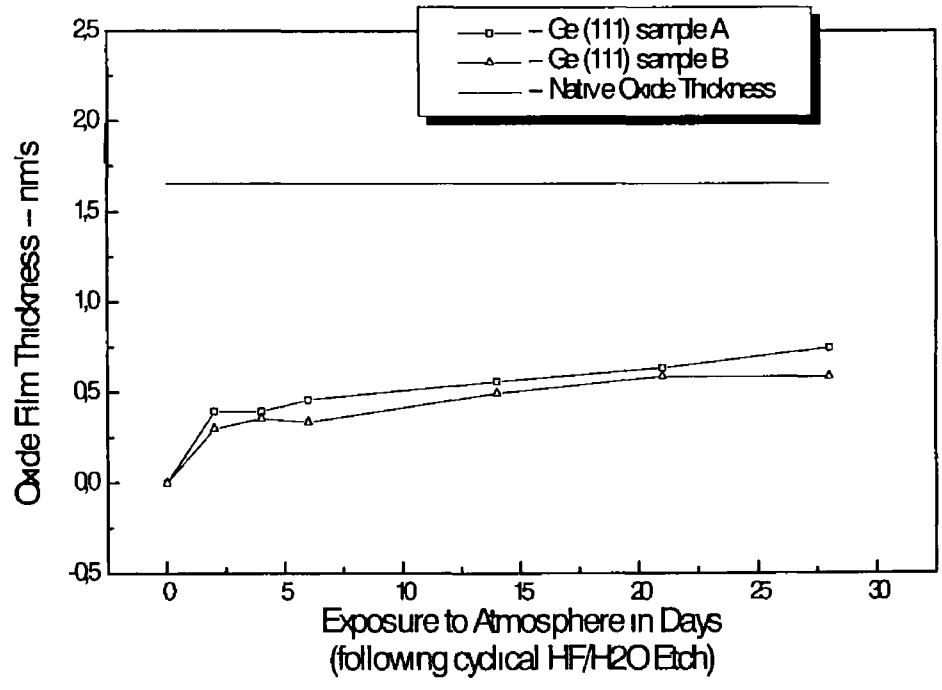

Figure 6 7 Oxide layer thicknesses calculated by the substrate/oxide ratio method for two HF/water etched Ge(111) samples with a native oxide for comparison

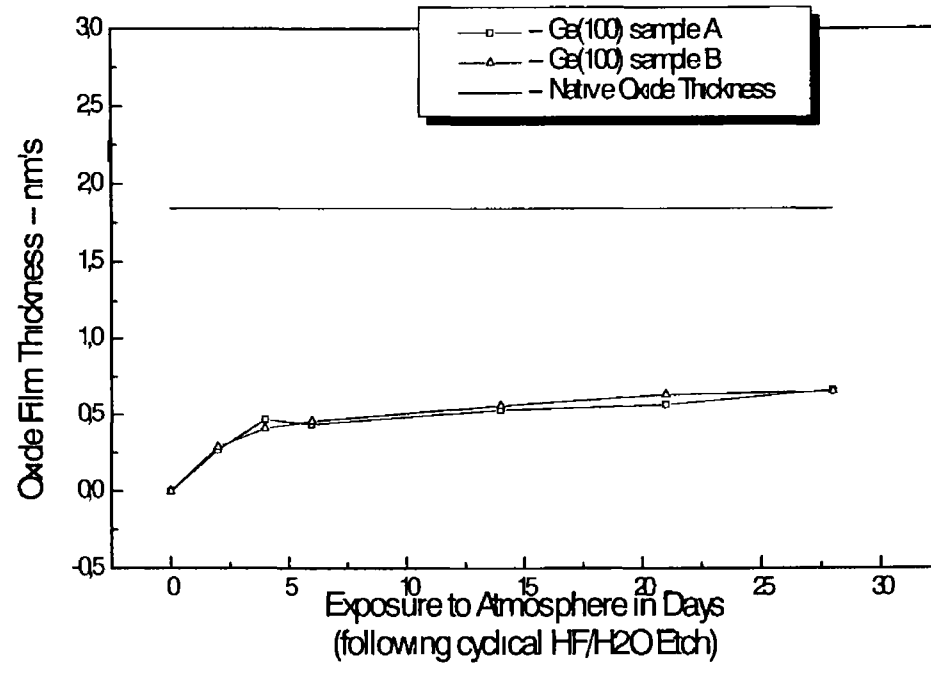

Figure 6.8 Oxide layer thicknesses calculated by the substrate/oxide ratio method for two HF/water etched Ge(100) samples with a native oxide for comparison

6.7 Discussion and Conclusions

Results clearly indicate that the described cyclical HF/water etching procedure for Ge surfaces, is a very effective oxide removal method In addition, the extremely slow rate of oxide regrowth under ambient conditions suggests that a Ge(111) surface prepared in this way is highly stable over extended periods of time An effective oxide thickness of between 0 6-0 8 nm after 28 days exposure to atmosphere indicates that this layer acts as an effective passivating layer preventing further oxidation of the surface No significant differences in the rate of native oxide regrowth were observed for the Ge(100) surface The regrown oxide thickness is substantially less that the native oxide thickness measured on a range of as received wafers as 2-3 nm In addition, the surface stability compares favourably with the results of a recent similar study of the ambient oxidation of the same two Ge surfaces prepared by a different wet chemical procedure [4] Their photoemission spectra displayed significant evidence of surface oxidation after just 6 hours exposure to air The results for Ge in the present study are comparable with those obtained recently for the ambient oxidation of hydrogen terminated Si(100) and Si(111) by Miura et al [13] They reported that the rate of oxidation of these surfaces strongly depended on the humidity of the air The ultimate oxide thickness from these studies on silicon 0.5-0 7 nm which are of the same order as the present investigation on germanium Both studies indicate that there is an initial high rate of surface oxidation which significantly slows after approximately 100 hr The slow regrowth of the native oxide gives reason to suggest that the Ge surfaces prepared in this way are predominately hydrogen terminated similar to the Si surfaces The hydrogen acts to passivate the Ge surface leaving it relatively unreactive in comparison to a surface not terminated in this way Figure 6 6 shows the contrasting regrowth rates between a HF/water etched sample and an argon ion bombarded sample which clearly cannot be hydrogen terminated After exposing both samples to ambient air conditions for 1 week the sputter-cleaned sample's oxide thickness is fast approaching the native oxide thickness whereas the HF/water etched sample is clearly resistant to ambient oxidation

Figure 6.9 : STM image of an untreated Germanium sample.

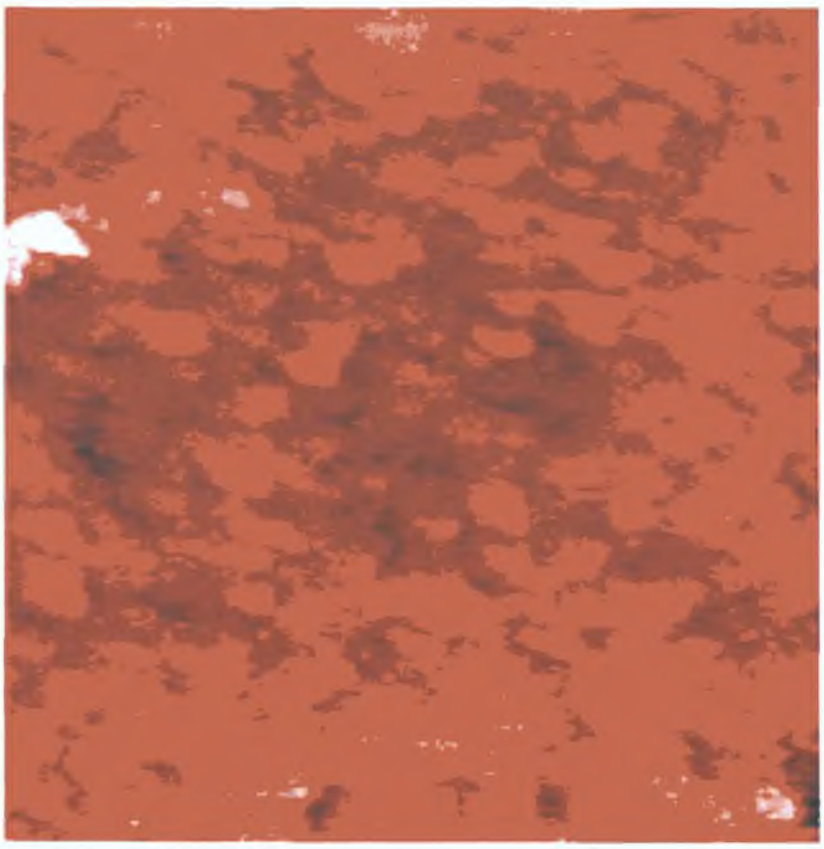

Figure 6.10 : STM image of HF / water etched Germanium sample.

Parameters	**Untreated Ge Sample**	**Etched Ge Sample**
Scan Size (in nm^2)	225	250
Height (in nm's)	15	7
Bias Voltage (in Volts)	-2	-2
Tunnel Current (in nA's)	1	1

Table 6.2 Scanning Tunnelling Microscopy (STM) scan parameters

Figures 6 9 and 6 10 are STM (Scanning Tunnelling Microscopy) images of the Ge surface taken before and approximately 1 hour after the HF/water etch procedure, respectively Following the HF/water etching procedure the STM image shows good surface flatness indicating that the etching procedure has not roughened the surface and further suggesting that the resistance to ambient oxidation is due to hydrogen termination of the Ge surface

These results are of significance to device fabrication procedures which involve the removal of the native oxide prior to subsequent processing They suggest that the HF treatment used is very effective at removing the native oxide and leaving the surface in a condition which is resistant to ambient oxidation

6.8 References

[1] J E Rowe, Appl Phys Letts 25(10) (1974) 576

[2] D Schmeisser, R D Schnell, A Bogen, F.J Himpsel, D Rieger, G Landgren and J F Morar, Surf Sci 172 (1986) 455-465

[3] C M Garner, I Lindau, J N Millar, P Pianetta and W E Spicer, J Vac Sci Technol 14 (1977) 372

[4] K Prabhakaran, T Ogino, Surf Sci 325 (1995) 263-271

[5] Y Wei, J L Sullivan and S O Said, Vacuum 45(5) (1994) 597

[6] X.J Zhang, G Xue, A Agarwai, R Tsu, M A Hasan, J E Greene and A Rockett, J Vac Sci Technol A11 (1993) 2553

[7] K Prabhakaran, T Ogino, R Hull, J C Bean and L.J Peticolas, Surf Sci 316 (1994) L1031-L1033

[8] S M Sze, Physics of Semiconductor devices (Wiley, New York, 1981)

[9] Unpublished Sulphur procedure developed by Sean Hearne, Physics Dept, D C U

[10] *See for example* M F Hochella and A H Carim, Surf Sci 197 (1988) L260-L268

[11] J Szajman, J G Jenkins, J Liesegang and R C G Leckey, J of Electron Spectrosc and Relat Phenom 14 (1978) 41

[12] H Gant and W Monch, Surf Sci 105 (1981) 217-224

[13] T Muira, M Niwano, D Shoji and N Miyamoto, J Appl Phys 78(8) (1996) 4373

Chapter 7 Conclusion

7.1 Introduction

The first objective of this project was to characterise an x-ray photoelectron spectroscopy system The system is based on the VG Scientific Clam100 spectrometer and is located at Dublin City University's, Physics department Accurate energy and intensity scale calibrations would allow quantitative surface chemical analysis studies to be carried out using the system

Once the system characterisation was completed, an XPS study of the removal of native oxides from the germanium (100) and Ge (111) surfaces was carried out It was found that the most effective wet chemical treatment to remove the native oxide, was a cyclical water rinse / HF etch Further work was also carried out on oxide re-growth rates and the apparent passivating effect of this thin regrowth layer

7.2 Calibration

Detailed energy and intensity scale calibrations were carried out by collecting calibration spectra for cleaned reference samples using the Clam100 system These spectra were then divided into standard reference spectra taken from the VAMAS (Versailles project on Advanced Materials and Standards) spectral library, to produce individual transmission functions for both x-ray sources (Mg Kα and Al Kα) of the Clam100 spectrometer

Frequent and careful system calibration, ensures that accurate quantitative information can be determined from XPS spectral data obtained using the spectrometer, for the various materials or surfaces to be studied

7.3 Thin film investigations on Germanium oxides

The chemical etching study on the germanium (100) and Ge (111) surfaces is presented in Chapter 6 The work began with the development of a cyclical water rinse / HF etch procedure, which was found to be the most effective oxide removal treatment of the various wet chemical treatments carried out The next stage was to establish an accurate method of determining the native oxide film thicknesses The method is based on consistently curve-fitting the chemically shifted components of the Ge 2p and Ge 3d core levels This method was also applied to the chemically treated Ge samples and led to the calculation of surface oxide re-growth rates on both the Ge (100) and Ge (111) surfaces

Oxide removal using argon ion bombardment revealed surfaces with substantial oxide re-growth, clearly showing the contrast between these Ge surfaces and the HF etched Ge surfaces, which indicate the re-growth of a very thin oxide layer

Comparisons between these thin film thicknesses (re-grown oxide layer) and literature values from similarly treated silicon samples, suggest that the etched Ge surfaces are hydrogen terminated This layer acts as an effective passivating layer preventing further oxidation of the surface and Ge surfaces prepared in this way are highly stable over extended periods of time STM (Scanning Tunnelling Microscopy) data of the Ge surface, taken before and after the water / HF etch treatment support the conclusion that the chemical etch used on Ge (100) and (111) samples resulted in the formation of hydrogen terminated surfaces and leads to the growth of a thin passivated surface layer

7.4 Final Remarks

The x-ray photoelectron spectrometer calibration and thin film investigations on germanium oxides were carried out as planned With the XPS study of the etching of native oxides on Ge (100) and Ge (111) surfaces yielding interesting results, suggesting the formation of hydrogen terminated surfaces Further work, in the area of surface ordering on etched Ge surfaces could be carried out in the future, using the LEED (Low Energy Electron Diffraction) technique and would be a valuable accompaniment to the investigation work as described in this thesis